Asymmetrical Subsidence Resulting from Material & Fluid Extraction

by

Patrick Martz

A THESIS SUBMITTED IN PARTIAL FULFILLMENT OF THE REQUIREMENTS FOR THE DEGREE OF BACHELOR OF APPLIED SCIENCE

in

GEOLOGICAL ENGINEERING

Faculty of Applied Science

Geological Engineering Program

Table of Contents

List of Figures

List of Tables

Abstract

Land subsidence has been experienced all over the world due to a multitude of natural processes and anthropogenic activities. Groundwater and material extraction both lead to subsidence at surface. Much of the literature related to subsidence evaluates parameters and modelling methods based on continuum derivations. These models often only simulate symmetrical profiles of subsidence because of assumptions of isotropy, homogeneity and continuum behaviour, when in many cases the geological conditions do not promote symmetry. The heterogeneity of the soil or rock mass and the presences of disconformities both contribute to difficult prediction of asymmetrical subsidence. Areas prone to subsidence are therefore of great concern as differential surface subsidence can compromise engineered structures. This paper focuses on the contributing factors of asymmetry in subsidence as observed in five industries: longwall mining, tunnelling, groundwater withdrawal, oil and gas extraction, and geothermal fluid withdrawal.

1. Introduction

The problem of ground subsidence spans a large variety of industries, from mining activity to oil and gas extraction to tunnel construction. When dealing with material extraction from the ground, subsidence will be a factor and must be accounted and designed for to prevent any unexpected, possibly harmful occurrence. Subsidence is described by Whittaker and Reddish (1989) as a downward vertical movement of a point which may include a horizontal shift of adjacent points caused by the original downward ground movement. It is not a new phenomenon, but is becoming an increasing concern as infrastructure and growing populations are increasingly affected by its occurrence.

1.1. Natural Subsidence

Ground subsidence occurs naturally and through anthropological means. In nature, tectonic or volcanic activities contribute to a lowering of the ground surface, for example, a large earthquake may cause the lowering of unconsolidated material. Whittaker and Reddish (1989) outline five ways in which natural subsidence can occur; soil compaction, soil shrinkage, lowering of the water table, development of subterranean voids by solution of host rocks, and tectonic and volcanic activities. These causes are important as they may be linked to the causes of subsidence during human development.

1.2. Industries that Generate Subsidence

As with natural subsidence occurrence, subsidence caused by industry projects often occur due to a lowering of the water table, extraction of fluids or ground loss. In general, any decrease in the strength or increase of the effective stress on the underlying rock or soil creates the potential for downward ground movement. Industries that extract fluids, including oil and gas, geothermal, and the use of groundwater for public water systems, all have the potential for surface subsidence. Industries which extract solid material from the ground, mainly mining and tunnelling (which at the same time tend to decrease the groundwater table through tunnel inflow) also lead to potential subsidence. Construction projects including the weight of buildings cause settlement of the ground surface due to soil compaction; however this type of subsidence will not be investigated in this thesis.

1.3. Problems Associated with Ground Subsidence

Whether surface subsidence occurs near an urban centre, on a coastline or in the middle of nowhere there is likely to be social, environmental or economic concerns generated, which underline the importance of studying and understanding it.

In urban centres, the structural strength of buildings can be severely compromised by a change in the elevation of the supporting foundation. This may result in a partial or complete failure of the building, a loss in property value or may even lead to human injuries or casualties. Since buildings are rigid

structures, differential settlement of the soil is especially troubling, as failure of the foundation at any point beneath the surface may cause partial failure of the building, thus, the prediction and monitoring of subsidence must be accurate.

Land subsidence of a larger area can be even more concerning, especially for cities situated along coastal waters. Venice and New Orleans are both examples of what can go wrong when subsidence occurs in a coastal region. Such a large area of subsidence is often attributed to both anthropogenic causes, mainly over pumping of groundwater from an underlying aquifer, and natural causes, including tectonic submersion and fault activity. The understanding of such activity is vital in order to predict and prevent (to a certain extent) large land submersions. Human reaction, in cases where a high maximum subsidence is unavoidable, is also important in such circumstances to prevent further socio-economic disasters, as happened with New Orleans.

Smaller economic issues also arise from the impact of subsidence in remote areas, primarily underground pipes and water lines that can be ruptured due to ground displacement. Occurrences such as this are problematic for companies, who may spend lots of time and money trying to find the right area in which a break may have occurred. This also lends itself to environmental and human health concerns if the pipeline contains oil or gas.

1.4. Magnitude of Structural Damage

Deformations of surface and sub-surface structures resulting from subsidence are dependent on many factors and in each case the tolerance of subsidence will

vary. Table 1 shows the severity of damage on structures due to tensile strains caused by differential subsidence. Table 2, in contrast to Table 1, shows the change of angular distortion (angular distortion is defined by as the ratio of differential settlement and the distance between any two points of the structure) due to subsidence, in relation to building type.

Class of damage	Change of length of structure	Description of typical damage
Very slight or negligible	Up to 0.1 ft (3 cm)	Slight cracks showing in walls and ceilings inside buildings, but not visible on outside
Slight	0.1 ft (3 cm) to 0.2 ft (6 cm)	Slight cracks showing inside the building; doors and windows will not close
Appreciable	0.2 ft (6 cm) to 0.4 ft (12 cm)	Slight cracks showing both outside and inside building; doors and windows will not close; drains, sewers, and gas pipes fracture
Severe	0.4 ft (12 cm) to 0.6 ft (18 cm)	Drains, sewers, and gas pipes fracture; open fractures through walls of building; window and door frames distorted, floors noticeably sloping, walls leaning or bulging noticeably; some loss of bearing of beams on walls; porticoes and floors buckle
Very severe	More than 0.6 ft (18 cm)	Worse than above and requiring partial or complete rebuilding; roof and floor beams lose bearing and walls lean badly and need external support; Windows broken and distorted; severe slopes, buckling, and bulging of roofs and walls occur

Table 1: Severity of damage on buildings due to change in length of structure caused by subsidence (Fang 1997).

Structure Class	Type of Structure	Limiting Angular Distortion
1	Rigid	Not Applicable
2	Statically determinate steel and timber structures	1/100 to 1/200
3	Statically indeterminate steel and reinforced concrete framed structures, load bearing reinforced brickwork buildings, all founded on reinforced concrete continuous and slab foundations.	1/200 to 1/300
4	As class 3, but not satisfying one of the stated conditions	1/300 to 1/500
5	Precast concrete large panel structures	1/500 to 1/700

Table 2: Limiting angular distortion (due to subsidence) dependent on structure type (Institution of Civil Engineers, 1977).

1.5. Data Recording and Prediction Methods

Prediction of surface land subsidence is extremely difficult for many reasons. For one, the ground underneath us is very complex. Adding to that complexity is the limitations we have for identifying subsurface profiles correctly. In order to predict accurately we must know the geology and geologic history of the subject area. Thorough site investigation must be undertaken to increase the likelihood that the description of the subsurface is acceptable. There are many advances in investigation techniques which have proved helpful. Geophysical surveys, borehole investigation, field tests and laboratory tests have improved the identification of faults, in-situ stresses, soil and rock classification and other anomalies that influence the ground response. However, these investigations are costly and as such may not all be utilized, depending on the budget, consequently

putting limits on the accuracy of what is known about the subsurface layers. Technological advances have also recently been made in recording the data of ground movements, which was originally accomplished by use of the levelling method, but now using GPS (Global Positioning System) and InSAR (Interferometric Synthetic Aperture Radar) the precise surface movement can be monitored using satellites. This also advances research as we can back calculate and model prior occurrences of subsidence very accurately.

The prediction of subsidence is often categorized into two different methods: either empirical or numerical methods. Empirical methods, including the profile function (Figure 1) and influence function, rely on previous studies of subsidence and are effective where initial data has been compiled, but are restricted since they do not take into account all geological conditions. Numerical methods use mathematical models and computers to predict subsidence occurrence. Though they are the most thorough subsidence prediction techniques, the ground conditions must be meticulously characterized in order for the techniques to work (Fang 1997).

Figure 1: Subsidence profile function (Fang 1997).

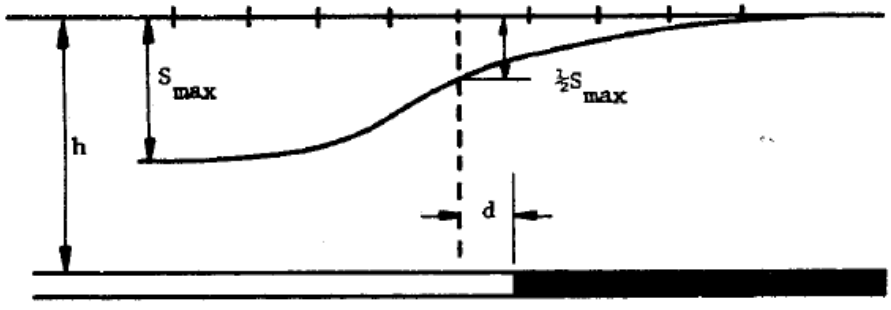

1.6. Asymmetrical Subsidence

Prediction of future subsidence frequently lends itself to simple solutions. Often the predicted and actual subsidence profile will be more or less symmetrical due to the assumptions inherent in the analysis and oversimplifications of the ground behaviour. However, the underground surface is not simple but instead very complex with different materials and different stress-strain responses, including planes of weakness such as faults and joints. These complexities can cause the surface subsidence to occur in such a way that it is not symmetrical, but is instead asymmetrical. In situations where the subsidence occurrence is different from the norm, it becomes exceedingly difficult to predict accurate future elevation changes in the general area, which heightens the risk of the social, economic and environmental issues outlined previously. This thesis will focus on identifying the major influences of what shapes the subsidence profile and which enact asymmetry in the following five industries; coal seam mining, tunnelling, groundwater withdrawal, oil and gas extraction and geothermal production.

2. Longwall Mining Subsidence

There are generally two types of subsidence (which are not mutually exclusive) caused by human activity: ground fluid withdrawal and material extraction. Longwall mining methods are of the second type as they extract large amounts of coal from beneath the earth. However, they may also contribute

to the first type since leakage into the mine and other hydrogeology effects may cause groundwater drawdown. This allows for many possibilities which may lead to unpredictable behaviour of the resulting subsidence.

In the late 1960's a study was conducted of the East Midlands Coalfield of the UK in which it was discovered that 25 percent of mining subsidence occurrences did not follow predicted results using standard prediction methods. It was concluded that geological factors must be accounted for where subsidence takes place (Whittaker and Reddish, 1989).

2.1. Flood Plain Effects

Mines are occasionally constructed beneath river flood plains which have variable water table heights. The change in the water table must be researched and monitored since the consequences of this variable may significantly impact subsidence in the area.

Another issue arising from an overlying flood plain is the gravels and alluviums at the surface, which lead to a different subsidence profile (Figure 2). As Whittaker and Reddish (1989) suggest, the unconsolidated wet surface deposits of the flood plain follow a slow gradual flow path towards the centre of the subsidence trough. The maximum subsidence has decreased in this case, but the border of ground disruption is farther reaching. This also results in a larger angle of draw, which Whittaker and Reddish (1989) showed were comparable with observations in the Netherlands.

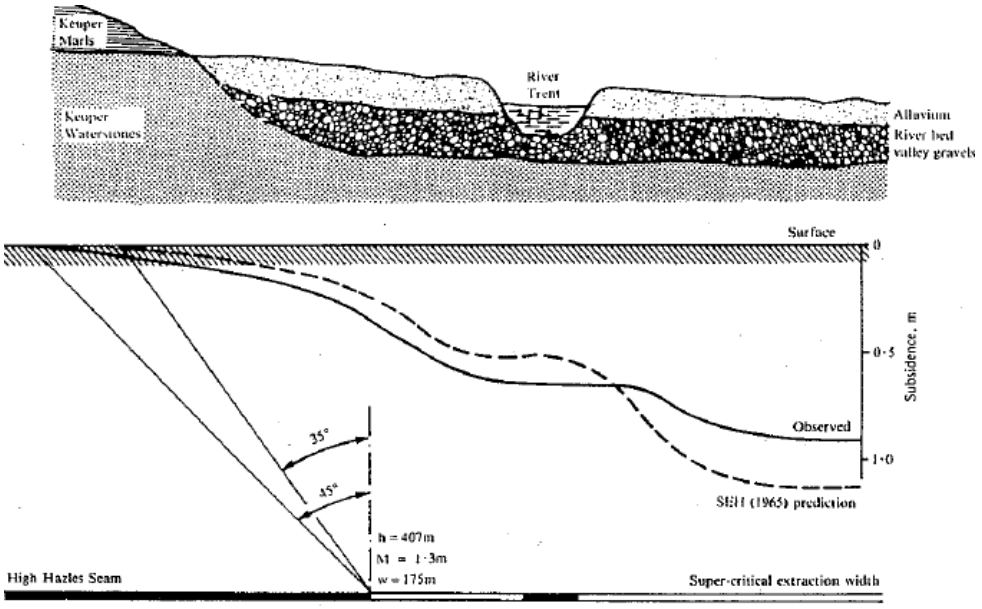

Figure 2: Flood plain effects on subsidence profile (Whittaker & Reddish, 1989).

2.2. The Effect of Near Surface Rocks and Joints

Prior to anthropogenic subsidence occurring above a coal mine, one must recognize the natural historic surface deformation that has already transpired. Surface rocks experience a number of natural events including folding, faulting and different stress distributions, which all contribute to the geomorphology of the area. As Whittaker and Reddish (1989) point out these factors need to be considered when studying subsidence behaviour. Ultimately, different types of rock that have

Figure 3: Separation of joints at the edge of the subsidence profile (Whittaker and Reddish, 1989).

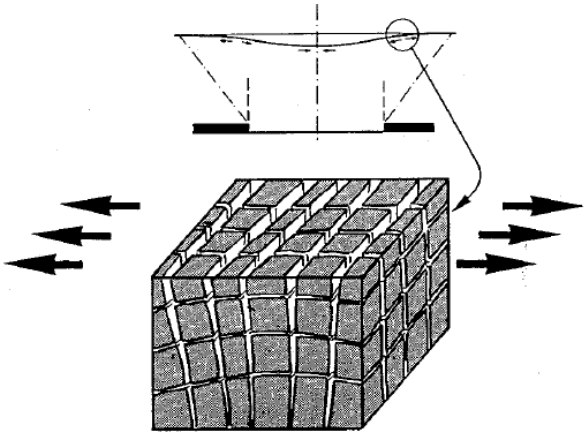

experienced different geological settings will behave differently when subjected to subsidence events. Joint patterns are one of the most important geological factors to be identified before an accurate prediction of subsidence can be made. According to Whittaker and Reddish (1989), under compression forces joints will not be susceptible to movement unless the strain is particularly high, however when joint patterns are subjected to tensile strain, which occurs on the edge of the subsidence profile (Figure 3), a separation may occur at the surface. Depending on the natural geological setting that exists in the area of concern, this separation of joints may result in block shear failure, slipping along joint planes, near surface bed separation leading to surface cracks, or fissures at the surface. Other than the obvious surface deformation (perhaps leading to structural damage of any buildings in the vicinity), the separation of joints can also affect the hydrogeological settings in the area. Groundwater flow patterns can change and increased local erosion may occur which can also lead to further subsidence at the surface, further accentuating the subsidence that has occurred due to material extraction. Fill material can also accumulate in the open fissures possibly leading to a dam of the water drainage system.

2.3. Hydrogeology

From the previous section, it follows that from jointing, bed separation and new fractures being created due to the extraction of material, that there will be a change in the hydrogeology of the area undergoing subsidence due to longwall extraction. There are likely to be two different responses to longwall extraction

by subsurface water systems. First, regions immediately surrounding the mine will be highly fractured which increases the hydraulic conductivity, eventually leading to dewatering and drainage into the mine. Second, there will likely be a different response by water closer to the surface, where there is a low-permeability aquitard present, preventing drainage of water, at a certain depth, into the mine. As Booth (2007) explains, there are several mechanisms which control the response of groundwater isolated from drainage into the mine in the case where subsidence persists: increased fracture porosity causing a potentiometric low in the subsidence zone; drawdown across the aquifer as water drains to the potentiometric low; increased fracture permeability reducing hydraulic gradients and lowering the water table upgradient; and drainage of aquifers into deeper aquifers through fractured aquitards. All mechanisms lead to a lower water table and pore water pressure, resulting in increased effective stress and consolidation. The increase of effective stress in the subsurface may lead to further more far reaching surface deformation, as the drawdown may occur in areas outside of the effected mine area if the drawdown is substantial. The existing geology is an important factor in the effects on groundwater as a higher transmissive unit can cause far reaching drawdown while a low transmissive unit (bedrock) will prevent drawdown outside of the subsidence area (Booth, 2007).

2.4. Coal Seam Angle

Coal seams are often aligned at angles, instead of lying flat. The geometry of the extraction that occurs from the angled coal beds produce asymmetrical

subsidence troughs as modelled by Alejano et al. (1999) in Figure 4. Alejano et al. (1999) model coal seams dipping at 60, 70, 80, and 90 degrees. At the dip of 60 degrees the subsidence trough shows obvious asymmetrical properties. As the coal seam dip goes to vertical, the subsidence trough become more symmetrical, leading to the conclusion that coal seam dip will influence the symmetry of the resulting subsidence profile.

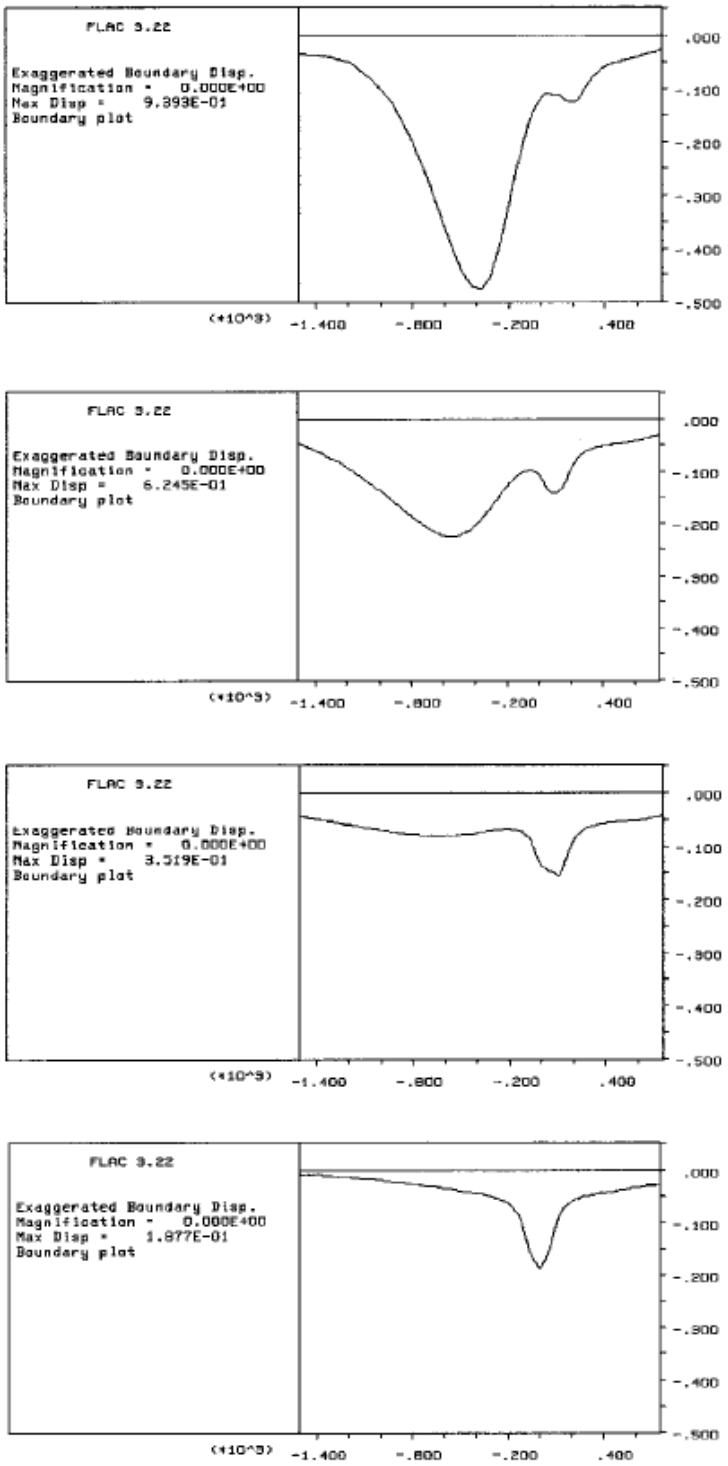

Figure 4: Subsidence troughs resulting from coal seams dipping at 60, 70, 80, and 90 degrees

2.5. Faulting

A fault occurring in the same vicinity as longwall subsidence can increase the development of surface deformation, as it increases the difficulty in predicting the behaviour of subsidence at surface and often leads to asymmetrical subsidence. There is also the possibility of fault reactivation, which may occur rapidly or over a long period even after subsidence has ceased. Conversely, a pre-existing fault may not be affected by local subsidence at all. However, the fault plane will be weaker than the surrounding rock which lends itself to slippage and displacement at surface, undermining engineered structures that may be present at the surface.

The response of a fault due to subsidence is largely dependent on a number of geological and mining factors. Donnelly et al. (2007) outline the geological mechanisms that influence fault response as: the stress field, geological history of the fault, geotechnical properties of the fault, proximity of the fault to the ground surface, hydrogeological conditions, and incidence and orientation of discontinuities in surrounding rock masses. The mining factors, also outlined by Donnelly et al. (2007) are: depth of mine from surface, mine and fault geometry, horizontal distance from the mine to the fault, rate of mining, thickness of the mine ore body, and the mining history. As there are many factors involved it is difficult to estimate exactly what will occur.

When the mine is terminated at the fault, depending on the orientation of each, the fault may act as a discontinuous boundary damping subsidence. This may lead to large differential settlement on surface with a step developing in the form of large strains stepping across the fault, as demonstrated in Figure 4. In such a

case, the subsidence profile will be dependent on the angle of hade (the angle between the fault plane and vertical) and the angle of draw (the angle from the vertical to the line stretching from the edge of the mine to the furthest point of subsidence at the surface, demonstrated in Figure 5). If the angle of hade is less than the angle of draw, subsidence will likely terminate at the fault, with a step or fault scarp at the edge of subsidence (Figure 5b). However, if the angle of hade is larger than the angle of draw, surface subsidence will likely extend to the fault at the surface (creating a wider subsidence profile as in Figure 5c). Additionally, other fault properties are pertinent for predicting to which degree they will affect the new stress and strain distribution. For instance, if the fault has a hade less than 30˚ with low frictional strength between its two faces and is of uncomplicated form, there will be a higher likeliness that the fault will experience a concentration of movement at the surface, resulting in a scarp.

Figure 5: Faults acting as subsidence control boundaries with several different orientations (Donnelly et al. 2007).

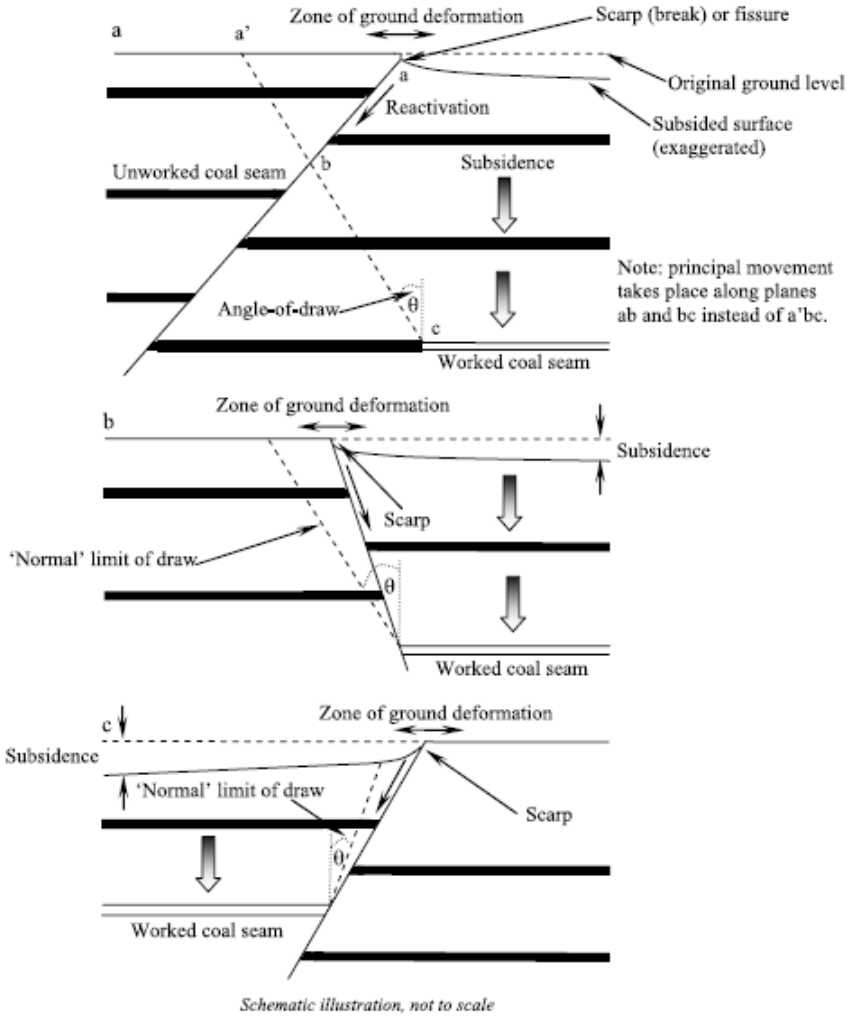

There are many other parameters that must be studied in order to identify how the surface will react when a fault is present during longwall mining. The surface geology is one of these important parameters. For instance, limestones and sandstones or other strong surface rocks tend to fracture and create blocks and more widespread damage and can lead to a reverse step (scarps usually face downwards towards where the material is being extracted). The fault may also lead to heavy fracturing and fissuring at the surface if it is located in a heavily

jointed deposit; in this case the fissures often run parallel to the fault. Thick ablation tills or other weaker surface ground may not be too loose to allow for an obvious fault scarp to reach the surface, or if a fault scarp does occur erosion may quickly erase any evidence other than a mildly elevated mound. Surface geology may play an important role in creating abnormal surface subsidence and can influence the magnitude of scarp development, thus should be investigated prior to mining.

Geotechnical properties of the fault are also very important when predicting fault response to subsidence due to longwall mining. The roughness, fill material, cohesion and porewater pressure of faults are properties that should be investigated. Roughness is often described quantitatively using JRC (Joint Roughness Coefficient, used in the Q-system of Barton et al. (1974)) or fractal geometry, and as Xie et al. (1998) suggest, should be the first step in studying fault influence on surface subsidence. The resistance of a fault to shearing is dependent on these parameters, but unfortunately as Donnelly et al. (2007) identify, difficulties with faulting in subsidence areas occur with the primary fault, which in most cases has experienced episodes of shearing and accordingly has a smaller degree of quantitative roughness (Xie et al. 1998).

All geological factors should be investigated before the commencement of any mining activity to lessen the effect of any mining factors that can arise due to poor practice. However, mining factors do occur regardless and must be taken into consideration. The most notable mine influence occurs when the material extraction takes place below the fault or on the footwall. The way in which strain

is released in this situation results in a higher likeliness of localized displacement and often a more pronounced scarp at the surface. Any scarp that may occur at the surface may have varying displacements, including some horizontal displacement, but generally in homogeneous ground the size of the scarp will remain constant, while the length of the scarp is related to the amount of extracted material, which is important in the prediction of such conditions. Fault scarps are also more probable in mine workings that are closer to the surface and where multiple seams of longwall mining take place. Once reactivation of a fault occurs, the displacement at the surface can develop disproportionately to the amount of extraction taking place, that is to say, small extraction may lead to a higher than normal scarp displacement (Donnelly et al. 2007).

Faulting may be one of the most important features in longwall mining subsidence as it produces abnormal subsidence profiles, including differential displacement at the surface, which is dangerous for engineered structures. Linear structures, such as roads, railways and pipelines are especially vulnerable to this displacement as they will probably cross the scarp at some point and be damaged. Agriculture and housing are also affected directly by surface subsidence, and indirectly by hydrological changes that may occur due to fault reactivation, as groundwater resurgence, leakage or disruption of drainage.

2.6. Prediction of Longwall Induced Subsidence

As stated in the previous sections, subsidence can be predicted using empirical, analytical or even physical methods. With the rise of technology, there

have been advances in prediction methods as we can now create computer programs to solve mathematical relationships, while the user simply inputs parameters collected from site investigations. While all of these parameters may be important to the shape and magnitude of subsidence, there will likely be only a few parameters selected for input into such programs to simplify and place importance on the most influential factors.

2.7. Case Study: Distinct Element Modelling of Southern Coalfields, New South Wales, Australia

Keilich et al. (2006) undertook distinct element modelling using the commercial code UDEC for the southern coalfields of New South Wales, Australia. In this study the authors used three different models to account for different width/depth ratios of the longwall mine (W/H ratios shown in Table 3). All geological units were accounted for in the study and their thicknesses from each model are shown in Table 4 and the geotechnical parameters of each unit are shown in Table 5. Bedding planes for all three models were assumed to be horizontal and had properties shown in Table 6. Joints were assumed to be vertical and the joint properties that were used are shown in Table 7. However they were not continuous instead forming non-continuous pattern through each layer. The bedding plane spacing was assumed to occur linearly with joint spacing in each lithological unit and is shown in Table 8. The joint normal stiffness and the shear stiffness are shown in Table 9 with the shear stiffness assumed to be one tenth of the joint normal stiffness. The horizontal to vertical stress ratio was

assumed to be 2.0 although investigation showed it could range from 1.5-2.0. Keilich et al. (2006) employed a Mohr-Coulomb elasto-plastic constitutive model in their analysis.

Table 3: 3 models analysed with different W/H (Keilich et al. 2006).

Model Name	Individual Panel Width W (m)	Cover Depth H (m)	Extracted Thickness (m)	W/H
Model 1	105	413	2.7	0.25
Model 2	158	450	2.5	0.35
Model 3	160	288	3.0	0.56

Table 4: Thickness of each lithological unit for each of the three models (Keilich et al. 2006)

		Model Name		
		1	2	3
Stratigraphic Unit Thickness (m)	Hawkesbury Sandstone	88	153	78
	Newport Formation	20	13	7
	Bald Hill Claystone	34	23	12
	Bulgo Sandstone	145	156	92
	Stanwell Park Claystone	40	23	11
	Scarborough Sandstone	50	32	36
	Wombarra Shale	16	29	29
	Coal Cliff Sandstone	20	21	23
	Bulli Seam	2.7	2.5	3
	Loddon Sandstone	8	8	8
	Balgownie Seam	1	1	1
	Lawrence Sandstone	4	4	4
	Cape Horn Seam	2	2	2
	UN2*	6	6	6
	Hargraves Coal Member	0.1	0.1	0.1
	UN3*	10	10	10
	Wongawilli Seam	10	10	10
	Kembla Sandstone	3	3	3
	Lower Coal Measures	50	50	50
	Total Depth	509.8	546.6	385.1

Table 5: Geotechnical parameters for each lithological unit. E = young's modulus, ν = poisson's ratio, c = cohesion, φ = friction angle, and σ_T = tensile strength (Keilich et al. 2006).

	E (GPa)	ν	c (MPa)	φ (°)	σ_T (MPa)
Hawkesbury Sandstone	13.99	0.29	9.70	37.25	3.58
Newport Formation	11.65	0.25	8.85	35.00	3.40
Bald Hill Claystone	10.37	0.46	10.60	27.80	2.90
Bulgo Sandstone	18.00	0.23	17.72	35.40	6.55
Stanwell Park Claystone	19.20	0.26	14.57	27.80	4.83
Scarborough Sandstone	20.57	0.23	13.25	40.35	7.18
Wombarra Shale	17.00	0.37	14.51	27.80	4.81
Coal Cliff Sandstone	23.78	0.22	19.40	33.30	7.87
Bulli Seam	2.80	0.30	6.37	25.00	0.84
Loddon Sandstone	15.07	0.33	17.10	28.90	5.65
Balgownie Seam	2.80	0.30	6.37	25.00	0.84
Lawrence Sandstone	15.07	0.33	17.10	28.90	5.65
Cape Horn Seam	2.00	0.30	2.87	25.00	0.70
UN2	13.48	0.25	19.89	28.90	6.74
Hargraves Coal Member	2.80	0.30	6.37	25.00	0.84
UN3	13.00	0.25	19.18	28.90	6.50
Wongawilli Seam	2.00	0.30	2.87	25.00	0.70
Kembla Sandstone	18.15	0.28	18.02	28.90	6.11
Lower Coal Measures	9.37	0.29	12.20	27.17	3.75

Table 6: Bedrock Properties (Keilich et al. 2006).

Property	Bedding Plane
Friction Angle (°)	28
Residual Friction Angle (°)	15
JCS	4
JRC	5
Cohesion (MPa)	0.7
Residual Cohesion (MPa)	0
Dilation Angle (°)	0
Tensile Strength (MPa)	0

Table 7: Joint surface properties (Keilich et al. 2006).

Property	Vertical Joint
Friction Angle (°)	28
Residual Friction Angle (°)	15
JCS	2
JRC	8
Cohesion (MPa)	1
Residual Cohesion (MPa)	0
Dilation Angle (°)	0
Tensile Strength (MPa)	0

Table 8: Bedding plane Spacing (Keilich et al. 2006).

Rock Unit	Bedding Plane Spacing (m)
Hawkesbury Sandstone	9
Newport Formation	1
Bald Hill Claystone	0.3
Bulgo Sandstone	9
Stanwell Park Claystone	3
Scarborough Sandstone	4
Wombarra Claystone	3
Coal Cliff Sandstone	3

Table 9: Joint normal stiffness and shear stiffness of rock units (Keilich et al. 2006).

Rock Unit	Normal Stiffness (GPa/m)	Shear Stiffness (GPa/m)
Hawkesbury Sandstone	21	2.1
Newport Formation	140	14
Bald Hill Claystone	204	20.4
Bulgo Sandstone	26	2.6
Stanwell Park Claystone	78	7.8
Scarborough Sandstone	76	7.6
Wombarra Claystone	115	11.5
Coal Cliff Sandstone	108	10.8

Figure 6 shows the results of the UDEC model for the second model. From this it was determined that slip along the bedding planes occur, and joint fissures occur along the edge of the goaf at surface. Table 10 shows the results of the analysis for each model. These models are in good agreement with observed subsidence in the southern coalfield. The model however does not predict the subsidence occurring in the Bulgo sandstone well, since this unit is believed to act as a massive elastic unit in which much of the subsidence is assumed to occur due to its warping.

Table 10: Final Results from UDEC prediction of all the models. Where $+E_{max}$=max tensile strain, $-E_{max}$=max compressive strain, Gmax=max tilt, T=Subsidence factor, K1=Max tensile strain constant, K2=Max compressive strain constant, K3=max tilt constant and D/H=position of inflection point relative to goaf. (Keilich et al. 2006).

Parameter	Model 1	Model 2	Model 3
W (m)	105	158	160
H (m)	413	450	288
T (m)	2.7	2.5	3.0
W/H	0.25	0.35	0.56
S_{max} (mm)	41.12	162.39	312.72
S_{goaf} (mm)	39.64	82.64	87.24
+ E_{max} (mm/m)	0.092	0.139	0.690
- E_{max} (mm/m)	0.065	0.287	0.516
G_{max} (mm/m)	0.086	1.275	3.731
D (m)	-96.00	5.50	18.50
S_{max}/T	0.015	0.065	0.104
S_{goaf}/S_{max}	0.964	0.509	0.279
K1	0.924	0.386	0.635
K2	0.653	0.794	0.475
K3	0.864	3.533	3.436
D/H	-0.232	0.012	0.064

Figure 6: Results of UDEC computation for Model 2 (Keilich et al. 2006).

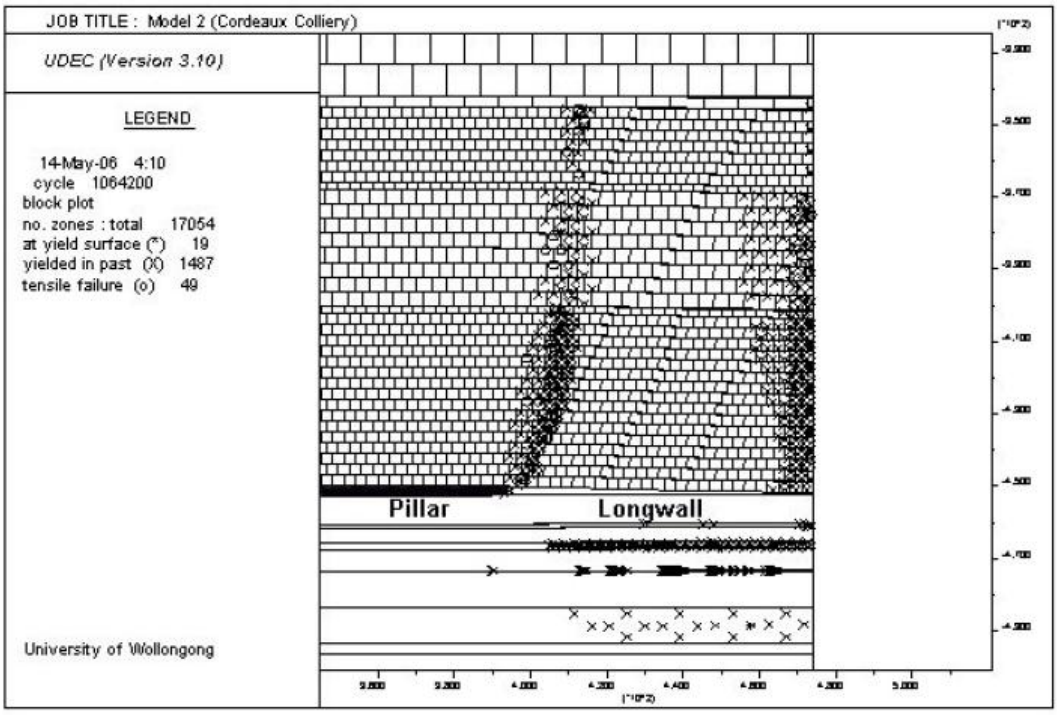

3. Subsidence Caused by Tunnelling

Tunnelling is likely to occur in a variety of areas with a variety of geological and structural obstacles for engineers to overcome, but in a different way than Longwall mining. Tunnelling may occur under a city, such as it did in London for the Jubilee Extension Line (Harris et al. 2000), where subsidence eventually caused officials to act in order to prevent the Big Ben Clock Tower from leaning over or possibly even collapsing. Conversely, tunnels may be built away from urban centres in alpine areas, such as the Gotthard Highway tunnel and base tunnel, where the effects of subsidence are may threaten the integrity of concrete dams or other strain sensitive infrastructure. Both soft rock and hard rock tunnelling will present a number of difficulties which must be dealt with and predicted to prevent certain differential subsidence from occurring.

3.1 Tunnelling in Soft Ground and Clays

Often tunnelling under cities for transportation routes or new utility lines involves soft ground. The major concern of course is tunnelling induced settlement that can occur under engineered structures. This may be through ground loss and/or drainage and consolidation of the soil. Advances in tunnelling technology have greatly increased in the last 30 years, for example the use of Earth Pressure Balance TBMs, however this does not mean subsidence is eliminated and in some cases when used improperly may even cause more. Empirical prediction techniques for such settlements have improved as well and three causes of settlement have been identified by Schmidt (1989): pore pressure

due to radial plastic displacement, excess face support pressure, and the tunnel acting as a drain. These causes can also be classified by the time scale over which they occur, as some may occur immediately while others are time dependent. The causes of these time dependent factors are displayed by Rankin (1988) in Table 11.

Table 11: Causes of time dependent factors of subsidence in soft ground tunnelling (Rankin 1988).

Displacement Phase	Nature of Loss	Cause of Loss
Initial	loss of material into the face;	elastic and/or plastic deformations and runs or flows of soil;
	loss over the shield;	police plates, over-cutters, or bead; over-excavation, ploughing, yawing or negotiating curves; pushing aside boulders; build up of grout on tailskin;
	loss on, or after, erection of lining (at tail);	when soil void not completely filled; delays in erection of lining or in grouting;
Time Dependent	loss with time as heading advances;	void collapse; lining deflection;
	additional loss with time;	volume decrease of soil; consolidation of soil,

Radial plastic displacement occurs where there is small internal supporting pressure resulting in a negative pore water pressure occurring around the tunnel, while a positive pore water pressure occurs at some distance away from the tunnel. This negative pore pressure occurs in the plastic zone that develops around the tunnel (which swells and can delay settlement) induced by the lack of support. The positive pore pressures at some distance will dissipate with time, leading to consolidation settlement. The subsidence trough at surface in such a case is wider than if this process had not occurred and the extent and magnitude of

subsidence is dependent on the size of the plastic zone (larger plastic zone creates larger subsidence trough). However, the effects of this are dependent on the construction method and pressure changes due to other tunnelling circumstances.

When using a tunnel boring machine that balances earth pressures (Figure 7), the face of the tunnel will often have a higher applied pressure than in-situ stresses. These high pressures in front of the tunnel cause positive pore pressures which may again lead to surface settlement.

Figure 7: Principle of an Earth Pressure balance machine (Leca et al. 2000).

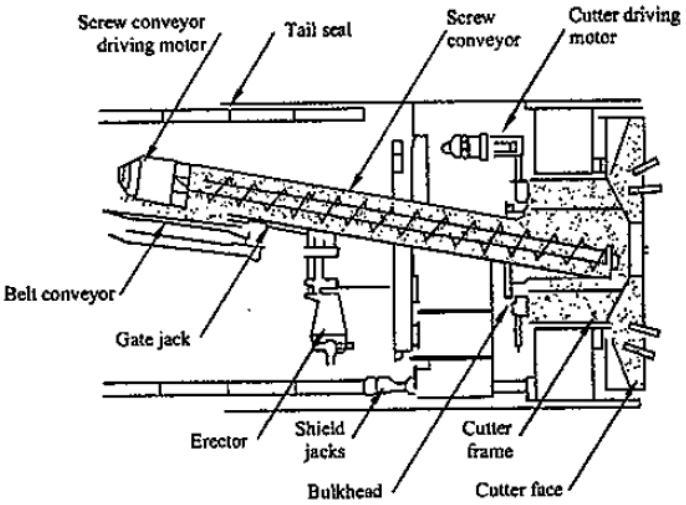

Subsidence of soft ground is also an issue where tunnelling occurs in fractured bedrock overlain by soils including clay deposits. Dewatering of the bedrock, such as happened in the Dayaoshan Railway Tunnel in China, will eventually lead to the dewatering of the shallower deposits. This will cause both subsidence of the bedrock as there will be less pore water pressure, and will cause settlement of the overlying deposits. In the case of the Dayaoshan Railway Tunnel, surface collapse features were found at 125 locations causing damage to buildings and utilities (Yuming 1998).

In order to predict subsidence phenomena occurrence good pre-tunnel site investigation is required. Classifying the soil, and predicting what may occur with settlement once tunnelling has commenced so that any settlement can be minimized (Shmidt 1989).

3.2 Tunnelling in Crystalline Rock

Significant subsidence in rock is usually reserved for highly porous sedimentary rock masses, however in some studies, such as the Gotthard Highway Tunnel in Switzerland, considerable subsidence can occur in fractured crystalline rock as well. The effect of this type of subsidence was not previously studied, as it's occurrence was unexpected and most research prior tto this study was focussed on soft rock over tunnels. However, there are a few exceptions, as the Gotthard tunnel (previously mentioned) has been thoroughly studied by Zangerl et al. (2008), as well Wu et al. (2004) studied inclined joint analysis in rock masses above tunnels.

Subsidence in crystalline rock will most likely occur in areas where the rock has horizontal or sub-vertical fractures. As Zangerl et al. (2008) point out, inclined fractures and brittle faults also allow for drainage to occur into the underlying tunnel rather rapidly. This leads to the conclusion that the subsidence occurring at surface is due to the closure of the fractured rock, since the pore water pressure has dropped, changing the stress distribution. Figure 8 shows the relationship between drainage into the tunnel and subsidence occurring at the surface. This redistribution of stress will lead to shear stresses forming in the

inclined joints, which ultimately can lead to slippage along the fractures when the frictional forces are overcome by the shear stress. This may also lead to dilation of fractures due to asperities preventing any vertical movement, though this dilation may be restrained leading to an increase in normal stress, thus changing mechanical and hydrological properties of the rock.

Figure 8: A) shows vertical displacement at surface, uplift from 1918-1970, subsidence from 1970-1993/98. B)shows drainage into the tunnel. Notice the correlation between the two (Zangerl et al. 2008).

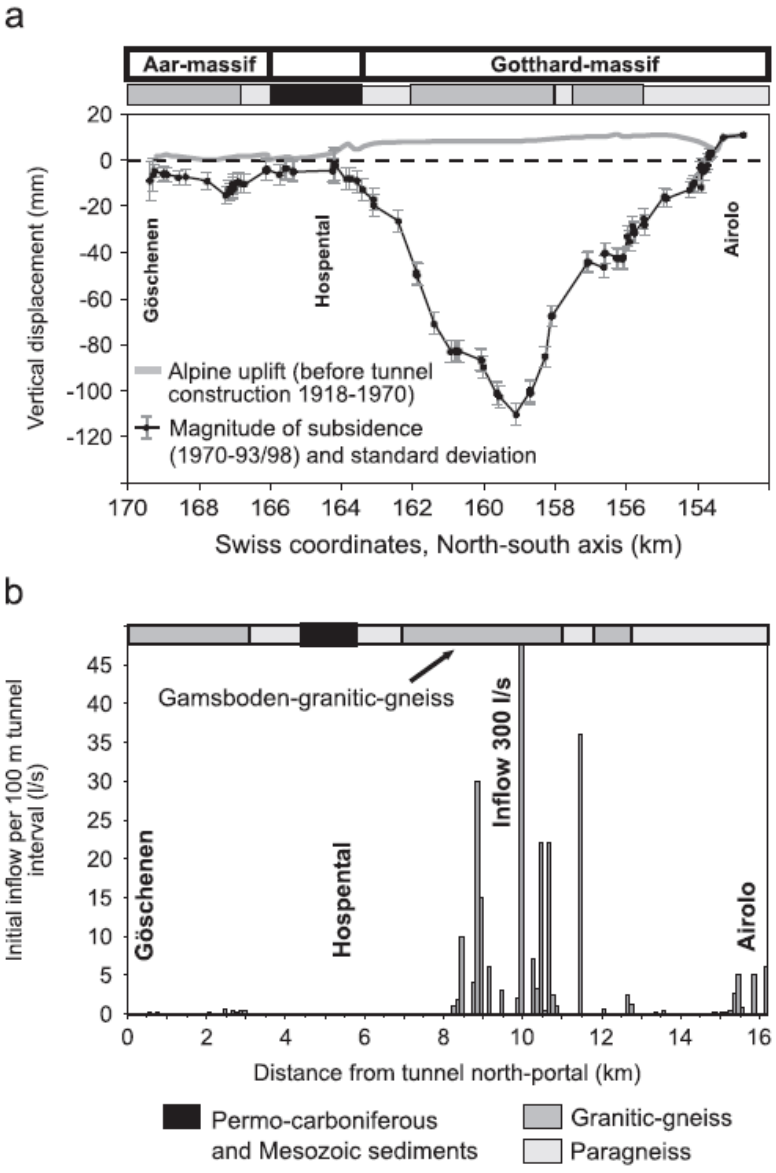

Zangerl et al. (2008) also suggest that there is a later mechanism that takes place leading to delayed subsidence. The mechanism is due to the much slower drainage of microfractures in the intact rock. The drawdown of water pressures in the fractures ultimately results in the drawdown of pore pressures in the intact rocks. The intact rock mass may contain some pore water and can result in further subsidence as the small fractures drain causing them to close due to the loss of pore water pressure. Though these microfractures are much smaller than the fractures and faults which originally allow groundwater to drain into the tunnel, they are still important considering the amount of rock volume involved. In the case of the Gotthard Tunnel the drainage from the small fractures in the large rock mass, although much more time dependent, eventually led to more subsidence, since the large scale fractures and faults are inclined and quickly drained upon intersecting with the tunnel (Zangerl et al. 2008).

Figure 9: Configuration of the Trap Door Test used to simulate subsidence in jointed rock. In Wu et al.'s test was completed with inclined angles of θ = 0, 30, 45, 60 degrees (Wu et al. 2004).

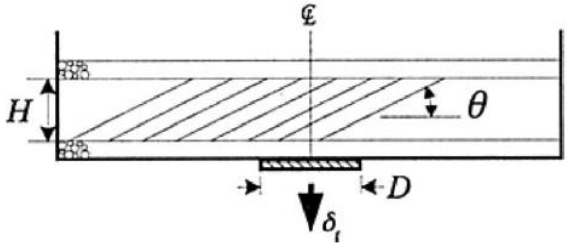

Wu et al. (2004) provide evidence that stress arching is also linked to surface subsidence in jointed rock masses, using the Trap Door (Figure 9) test and Discontinuous Deformation Analysis (DDA). Stress arching occurs in a tunnel when the support or rock block deforms, but does not yield in failure; instead shearing resistance of the surrounding rock and support carries the rock load.

This disruption in stress causes a concentration of vertical stress around the deformed block which leads to subsidence at the surface. Furthermore, the inclination of the joint angles significantly affects the shape of the surface subsidence. If the inclined angle (shown in Figure 9) is at 0˚ the subsidence profile will be symmetrical, however as the angle becomes more inclined the subsidence profile will become asymmetrical. Figure 10 from Wu et al. (2004) shows the different subsidence profiles that occur with changing angle of joints.

Figure 10: Dip angle of joints/faults of A) 0˚ B) 30˚ C) 45˚ D) 60˚ (Wu et al. 2004).

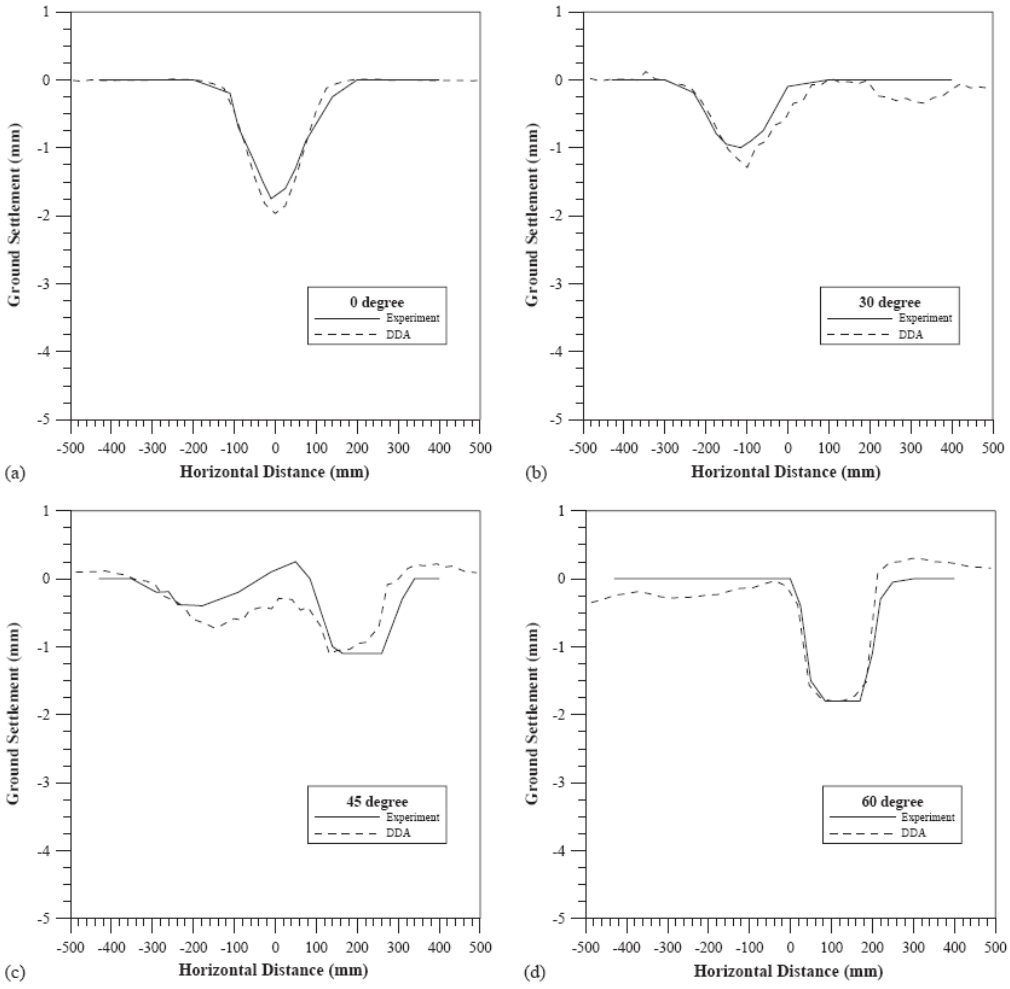

3.3 Tunnel Subsidence Prediction

Prediction techniques for tunnelling are similar to that of longwall mining. The advancement in computers has produced a simpler way to use mathematical models in order to predict future subsidence. However, it is still very difficult to predict with only a few simplified parameters, since there are so many other influential characteristics. Add to that the fact that some parameters that are needed cannot be known until tunnelling has commenced.

Of the analytical and empirical methods used to predict subsidence in tunnelling the Peck (1969) method is one of the most common for soil. This method however is based on prior experience and does not take into account new tunnelling techniques such as the shield techniques. Accordingly, there are many other prediction methods as outlined by Melis (2002). These include the Sagaseta Method, the Verruijjt-Booker Method, the Oteo Method, and the Loganathan-Poulos method.

3.3.1 Peck Method

The Peck Method, later improved by Atkinson and Potts (1977) and Clough and Shmidt (1981) used the following equations:

[1] $$\delta_z(x) = \frac{V_S}{i\sqrt{2\pi}} \exp\left(\frac{-x^2}{2i^2}\right) = \delta_{z,\max} \exp\left(\frac{-x^2}{2i^2}\right)$$

Where $\delta_{z,max}$ is the maximum settlement of the tunnel axis, x is the distance from the centreline, *i* is the point of inflection of the normal subsidence curve, and V_S is the volume loss between the original ground surface and the subsidence trough

per metre of tunnel advancement. V_S is correlated by Peck (1969) with the stability number N, which is given by (after Broms and Bennermark, 1967):

$$[2] \qquad N = \frac{\sigma_v - \sigma_T}{s_u}$$

Where σ_v is the total vertical stress at the tunnel axis, σ_T is the internal support pressure, and S_u is the undrained shear strength of the soil. The *i* values are also often found by the equation (Sagaseta et al. 1980):

$$[3] \qquad \frac{i}{R} = \eta\left(1.05\frac{H}{D} - 0.42\right)$$

Where R is the radius of the tunnel, η is a parameter dependent on the soil, H is the tunnel axis depth and D is the tunnel diameter.

3.3.2 Oteo Method

The Oteo method uses the equation (Oteo and Moya 1979; Sagaseta et al. 1980):

$$[4] \qquad \delta_z = \Psi\frac{\gamma D^2}{E}(0.85 - \nu)\exp\left(\frac{-x^2}{2i^2}\right)$$

Where *v* is poisson's ratio, *γ* is the total unit weight of the soil, Ψ is an empirical parameter from evaluation of monitored data and *E* is the extension Young's Modulus. *i* is obtained through equation [3] above.

3.3.3 Sagaseta Method

The Sagaseta Method takes ovalization (Figure 11) deformation of the tunnel into account and employs the following formula (Gonzalez and Sagaseta 2001):

$$[5] \qquad \delta_z(x) = 2\varepsilon R\left(\frac{R}{H}\right)^{2\alpha-1}\frac{1}{(1+\bar{x}^2)^{\alpha}}\left(1+\rho\frac{1-\bar{x}^2}{1+\bar{x}^2}\right)$$

Where ε is the radial strain given by $\varepsilon = V_s/2$, ρ is the relative ovalization given that $\rho = \delta/\varepsilon$ (where δ is the ovalization), $\bar{x}$ is the relative distance to the tunnel axis given by x/H, and α is a parameter to account for volumetric strains in the plastic range.

Figure 11: Ovalization deformation of a tunnel (Maynar et al. 2005).

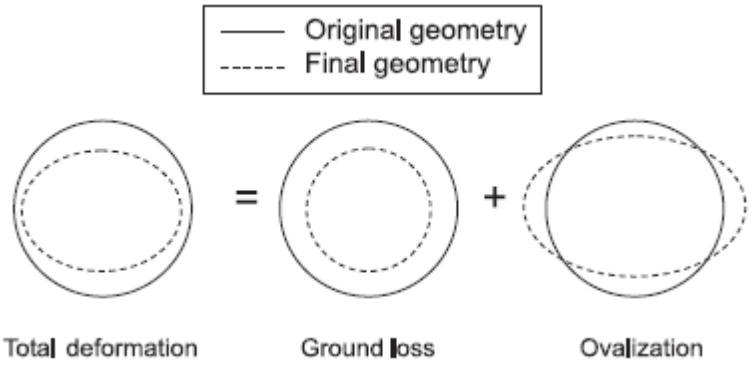

3.3.4 Verruijt-Booker Method

This method is a generalization of the Sagaseta method and is defined by (Verruijt-Booker 1996):

$$[6] \qquad \delta_z(x) = 4\varepsilon R^2(1-\nu)\frac{H}{x^2+H^2} - 2\delta R^2\frac{H(x^2-H^2)}{(x^2+H^2)^2}$$

All parameters have been defined previously. In this case however, ε is given by: $\varepsilon = V_S/4(1-\nu)$.

3.3.5 Loganathan-Poulos Method

This method is given by (Loganathan and Poulos 1998):

$$[7] \qquad \delta_z(x) = (1-\nu)\frac{H}{x^2+H^2}(4gR+g^2)\exp\left\{-\left[\frac{1.38x^2}{(H+R)^2}\right]\right\}$$

Where g is the undrained gap parameter and is given by $g = G_p + U_{3D} + \omega$; Gp represents the gap between the skin of the shield and the lining of the tunnel, U_{3D} is the elasto-plastic deformation of the tunnel face and ω is the parameter defining the quality of the tunnel's workmanship.

3.4 Case Study: METROSUR Extension Project

Located southwest of Madrid, Spain, this transportation expansion was built as a circular network connecting with the Madrid Metro Network. It connects 5 cities (Figure 12) and saw 150,000 people use it in its second day. The tunnel was built with a closed face EPB machine.

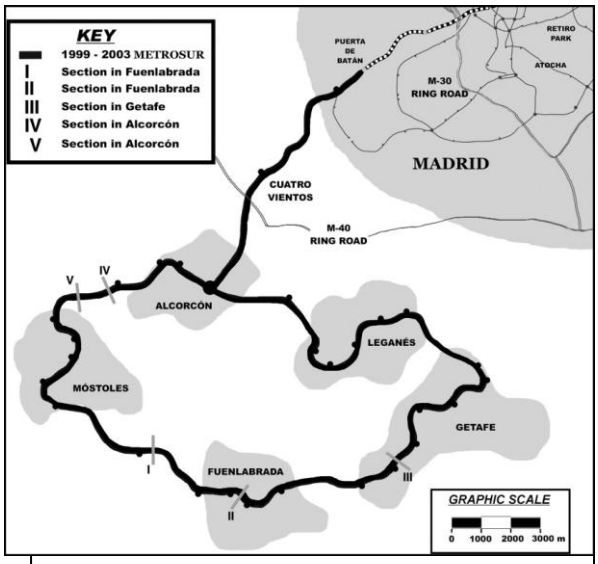

Figure 12: METROSUR Extension Project. (Melis et al. 2002)

Melis et al. (2002) thoroughly studied the affect of the tunnel on the surface, and made attempts to predict subsidence using the prediction methods listed above. They also did each prediction using information gathered at five different areas in which the tunnel was being constructed, however, in this thesis only section III will be discussed.

Table 12: Values estimated for each prediction method (Maynar et al. 2005).

	Peck		Oteo						Verruijt–Booker				Loganathan–Poulos		Sagaseta		
Section	*i* (m)	V_S (%)	η	γ (kN/m^3)	*i* (m)	Ψ	*E* (kPa)	ν	ε (%)	ρ	δ (%)	ν	*g* (m)	ν	ε (%)	ρ	α (%)
I	6.3	0.50	1.13	20.2	6.3	0.3	467	0.30	0.18	1.3	0.23	0.30	0.012	0.30	0.25	1.3	1
II	7.5	0.35	1.07	20.1	7.5	0.3	420	0.31	0.13	1.3	0.17	0.31	0.012	0.31	0.18	1.3	1
III	9.5	0.23	1.13	20.4	9.5	0.3	374	0.29	0.08	1.3	0.10	0.29	0.012	0.29	0.12	1.3	1
IV	4.5	0.70	1.30	20.2	4.5	0.7	600	0.29	0.25	1.3	0.33	0.29	0.012	0.29	0.35	1.3	1
V	4.5	0.25	1.24	20.3	4.5	0.3	551	0.30	0.09	1.3	0.12	0.30	0.012	0.30	0.13	1.3	1

Section III was located in Getafe, it had an overburden of 12.8 metres and comprised of several man-made fills, sandy clays, and highly plastic clays. Figure 13 is the cross-section of the studied area. The estimated parameters needed for the prediction using the above prediction techniques are shown in Table 13. Only section III pertains to this overview however.

Figure 13: Cross-section of Section III (Maynar et al. 2005).

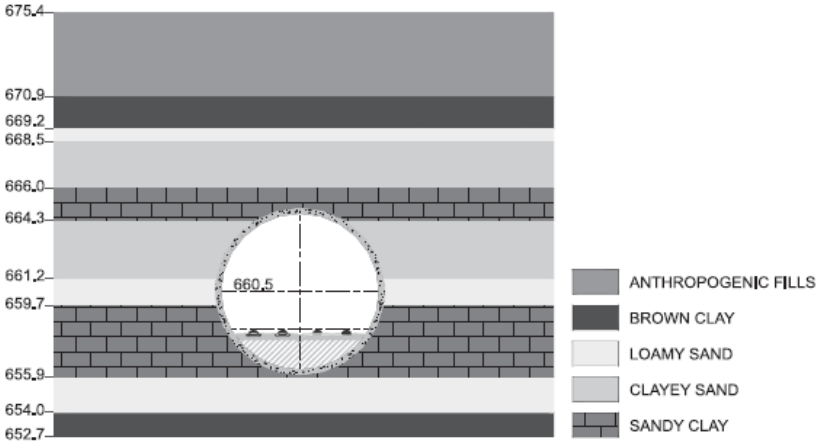

The resulting subsidence profiles from the prediction techniques are shown in Figure 14, along with the actual measured data after the construction of the tunnel was complete. The profiles show that the best prediction technique for this area was Sagaseta and Verruijt, while the other methods were far too conservative. The maximum subsidence of the trough was -4.4 mm while the max from the Sagseta method was -4.6 mm. On the other extreme, Peck had a subsidence trough depth of -11.1 mm. All models, however, failed to predict the

asymmetry of the subsidence profile, as the real data shows that the profile is wider on the right. The models used to predict the subsidence are fundamentally symmetric, thus would not be able to account for any possible differences on either side of the profile. The researchers of this study, Maynar et al. (2005), could not find any explanation for such asymmetric behaviour other than the possibility of a heterogeneous geotechnical profile. Overall, the prediction methods did a poor job of predicting the subsidence profile; this is mainly due to the fact that they do not account for continuous grouting of the gap as the shield advanced eliminating ground loss, the workmanship was of better quality than originally assumed, and these predictive techniques do not take into account the effect of buildings, roads and foundations which constrain soil movement (Maynar et al. 2005).

Figure 14: Predicted subsidence profiles and actual monitored data (Maynar et al. 2005).

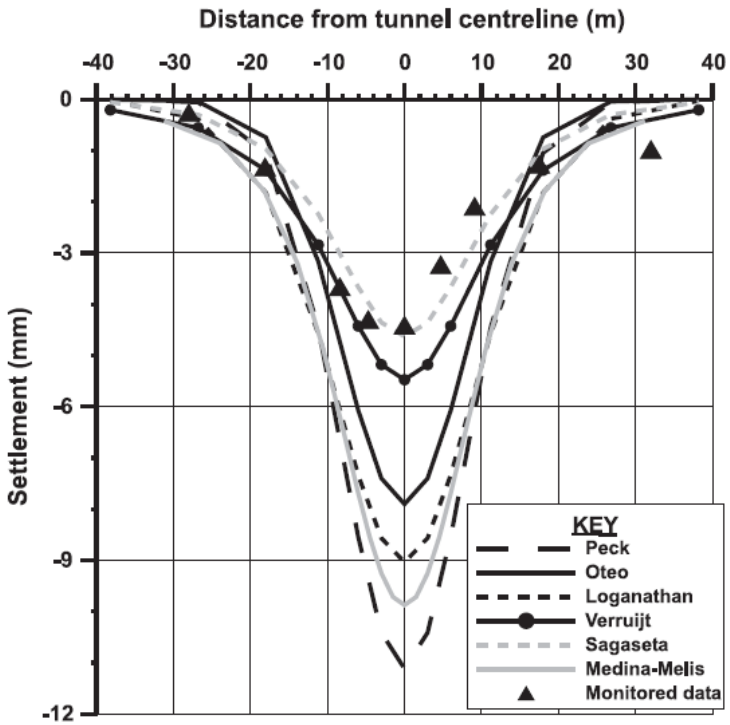

4. Subsidence Caused by Groundwater Withdrawal

Subsidence in the case of groundwater withdrawal is very different from the previous section of solid extraction, however there are similarities. For instance, longwall mining and tunnelling both result in groundwater drawdown due to drainage into the opening created by solid extraction, which was one of the mechanisms that lead to surface subsidence. Many urban centres rely on groundwater for a variety of reasons, such as agriculture and drinking water. This need for groundwater can cause overpumping, where the extraction exceeds recharge of the underlying aquifer over a certain period of time, as Figure 15 illustrates. Aquifers are highly permeable unconsolidated soil that allow fresh water to flow through them and are accompanied by aquitards which are made of fine grained soils, such as clays. It is the aquitards that are very porous, usually normally consolidated clays, and thus are very compressible when water is drawn out of them. An example of a confined aquifer and aquitard system is shown in Figure 16. In the United States, groundwater accounts for around 80% of all subsidence occurrences (Thompson 2006).

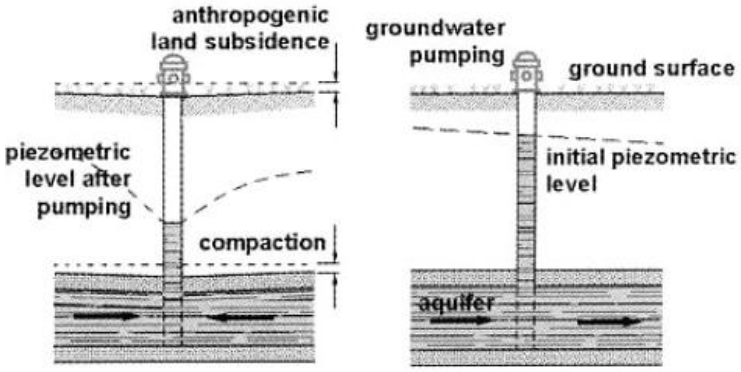

Figure 15: Resulting drawdown from overdraft of groundwater reservoir over time (Gambolati et al. 2006).

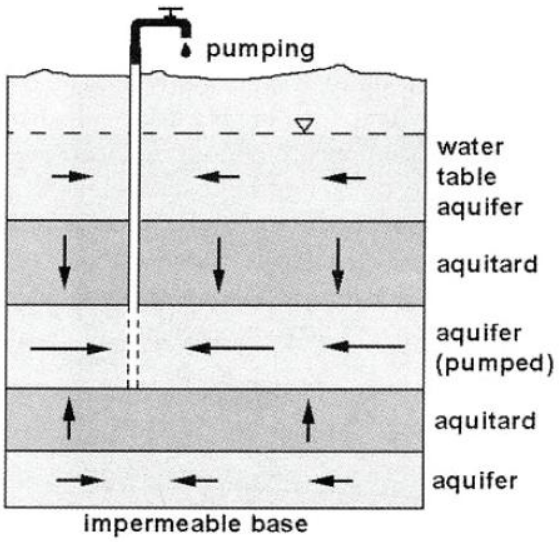

Figure 16: An aquifer/aquitard system (Gambolati et al. 2006).

Groundwater subsidence occurs because of the redistribution of stresses. This is explained by Terzaghi's principle of effective stress, as drawdown occurs the pore water pressure will decrease in the area. This will cause an increase of effective stress which the soil will have to bear; eventually the stress on the soil will be great enough to cause it to consolidate, creating subsidence at surface. The long term results of subsidence will depend on whether the deformation that occurs is elastic or inelastic. In the case of elastic deformation, if the water is restored then the land will rebound. However in the inelastic case, when the soil has reached and gone beyond its elastic limit, the subsidence is permanent and will also limit the amount of water the soil can store or the storage coefficient. The inelastic deformation usually occurs in the aquitard, as water will seep out of the compressible layer causing a decreased irreversible volume. The degree and occurrence of subsidence will rely on the geological properties of the subsurface, the mechanical behaviour of stratified units and the amount and area of

groundwater extraction (Zhang et al. 2007). However, there are other factors that can influence the shape and vertical displacement of groundwater subsidence, such as the thickness of the aquifer, interlaying sub-layers and groundwater level and flow (Mousavi et al. 2001).

An example of groundwater withdrawal induced subsidence occurs in California near Mendota in the San Juaquin valley. Figure 17 shows the different ground levels from 1925 to 1977 near the location of maximum subsidence for the valley which was found to be greater than 28 feet in 1970 (Galloway et al. 1999). The areal extent of the subsidence of this valley is also large as 5 200 miles experience subsidence greater than 1 foot, which could cost building owners however most of the land is agricultural. The subsidence of this area is due to groundwater pumping for mostly agricultural use. Since 1970 subsidence has slowed as groundwater pumping has been reduced allowing for groundwater levels to recover. The large amount of subsidence taking place here is largely attributed to the deposits filling the valley, as half of the continental sediments are silts and clays vulnerable to compaction when groundwater drawdown occurs (Figure 18) (Galloway et al. 1999). This example shows the large area and depth that groundwater withdrawal caused subsidence can incur on a valley filled with compressible soils and shows the importance of studying this type of subsidence.

Figure 17: Mendota, California subsidence due to groundwater withdrawal from 1925 – 1977 (Galloway et al. 1999).

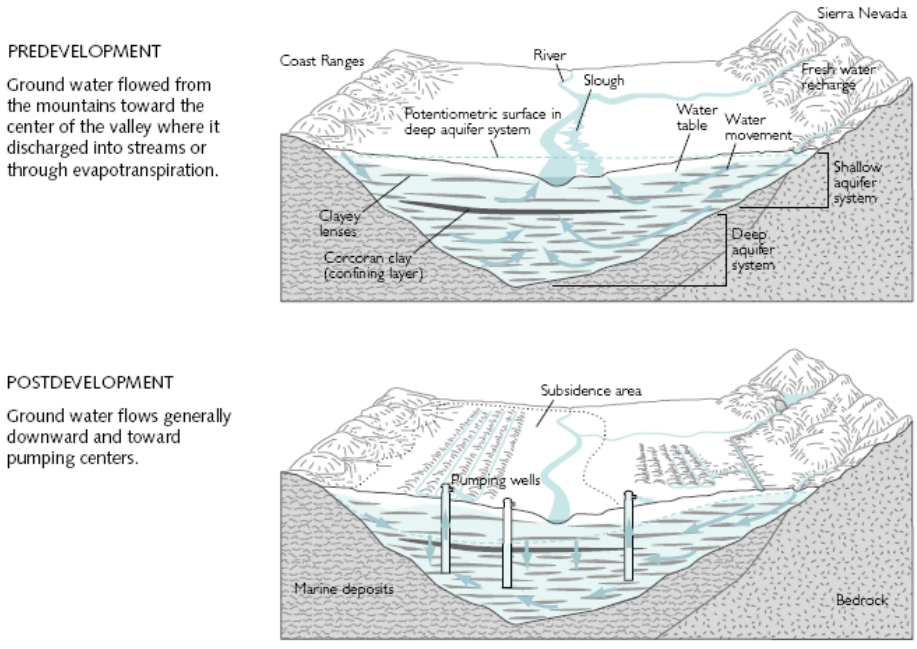

Figure 18: Cross-section predevelopment and postdevelopment of the San Juaquin valley (Galloway et al. 1999).

4.1 Soil and Rock influence on Groundwater Subsidence

Until this point in this thesis the occurrence of subsidence has been linear, following the path and footprint of either a longwall mine or a tunnel. Groundwater subsidence differs since the extraction of water is produced at a point source, not along a line. This will affect how the subsidence will occur on surface. Since the drawdown of groundwater will be in the shape of a cone of depression, the subsidence will be prone to follow the area of drawdown creating a bowl shaped subsidence profile in three dimensions. Depending on the rate of subsidence, drawdown could extend significantly away from the point of extraction, thus leading to subsidence in areas distant from the point source. In areas of large groundwater production, with many wells, the aquifer from which the wells are producing will likely see its average groundwater table decline as the several cones of depression coalesce, which can lead to subsidence at the surface above the entire extent of the aquifer. Conversely, subsidence may also be limited by impermeable barriers.

Soil and rock conditions are very influential in the shaping of surface subsidence. Heterogeneity and anisotropic conditions can cause varied results, especially in three dimensions. Hydrostratigraphic units can have a variety of different responses with differences in time and space. For instance, Zhang et al. (2008) explain that the subsidence experienced due to groundwater withdrawal in Shanghai exhibited different mechanical behaviours based on different changing patterns of piezometric level, which may be expected, but there were also

discrepancies of subsidence behaviour due to the vicinity to the centre of the cone of depression. As shown in Figure 19, the piezometer close to the edge of the cone of depression (Figure 19A) experienced compaction linearly with the rise and fall of the piezometer level through 1989-2002, while the piezometer at the centre of the cone of depression (Figure 19B) experienced continuous compaction even though the piezometer level trended upwards from 1990-2003. Towards the end of this trial the curve turned sharply upward then to the left, indicating the elastic expansion caused by the increased piezometric level was almost compensated for the continuing compaction at first, then expansion exceeded compaction as there was overall uplift after 2002. This discontinuous subsidence shows a few of the mechanisms that can affect the overall shape of subsidence from groundwater withdrawal.

Figure 19: A) Cumulative compaction vs. Piezometric level from 1989-2002 in Shanghai at edge of cone of depression of second aquifer. B) Cumulative compaction vs. Changing piezometric levels from 1990-2003 in Changzhou at the centre of the cone of depression in second aquifer (Zhang et al. 2007).

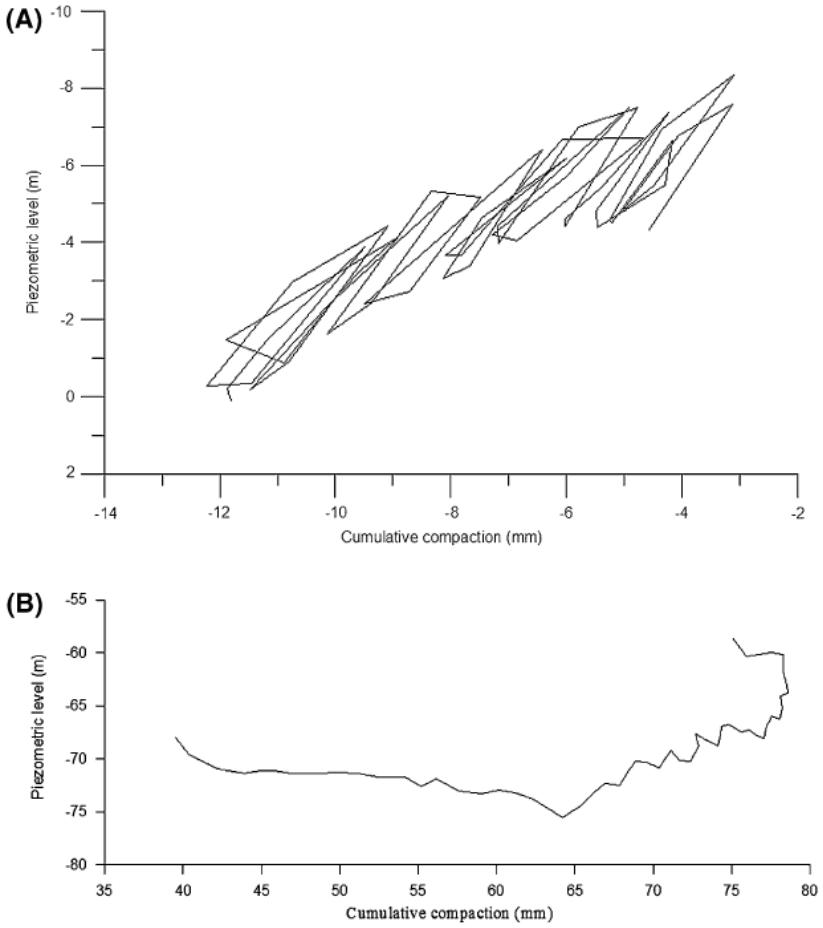

As stated previously, the bowl of subsidence often follows the cone of depression of groundwater with the maximum subsidence occurring approximately at the centre of the cone of depression. This will occur when extraction is related to just one aquifer. However, as Zhang et al. (2007) reports, this is not the case where large amounts of extraction occur from different aquifers. In Shanghai, a significant amount of groundwater was extracted from the second and third aquifer cross-section of aquifers (shown in Figure 20), causing the zones of depression and subsidence to not align as they would

normally. Zhang et al. (2007) refer to aquifer thickness, the texture and compressibility of the hydrostratigraphic soil, and the changing levels of piezometers as the factors which cause subsidence and groundwater depression not to line up. Furthermore, this can lead to asymmetry occurring at surface when viewing the subsidence profile. These multi-layered aquifers will each contribute a certain amount of subsidence dependent on the factors outlined by Zhang et al. (2007), when water is extracted from the different layers, as is shown in Table 13 in the case of Shanghai. From the table it is evident that the first aquitard is the most compressible (also proven by samples) while the deeper aquitards have low to moderate compressibility, which is especially evident in the 1980's. However, in the 1990's all layers had a piezometric low causing all to have significant compaction. The third layer in this case created the highest percentage of compaction because of its thickness, giving way to visco-elasto-plastic compaction and increased in compaction more rapidly. Conversely, at group FQL, the second aquitard was the most influential layer causing subsidence because from the second aquifer most groundwater was extracted in this area. As this study by Zhang et al. (2007) describes, the shape and extent of subsidence at the surface, which follows the subsidence rates shown in Figure 21, will be the product of many different factors in time and space, any of which can cause the subsidence bowl to become asymmetrical.

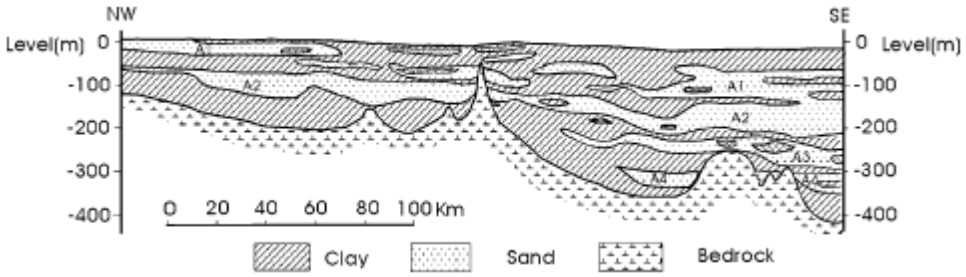

Figure 20: Aquifers of the Southern Yangtse Delta (where Shanghai is located. A1=First aquifer, A2=Second aquifer, A3=Third aquifer and A4=Fourth aquifer (Zhang 2007).

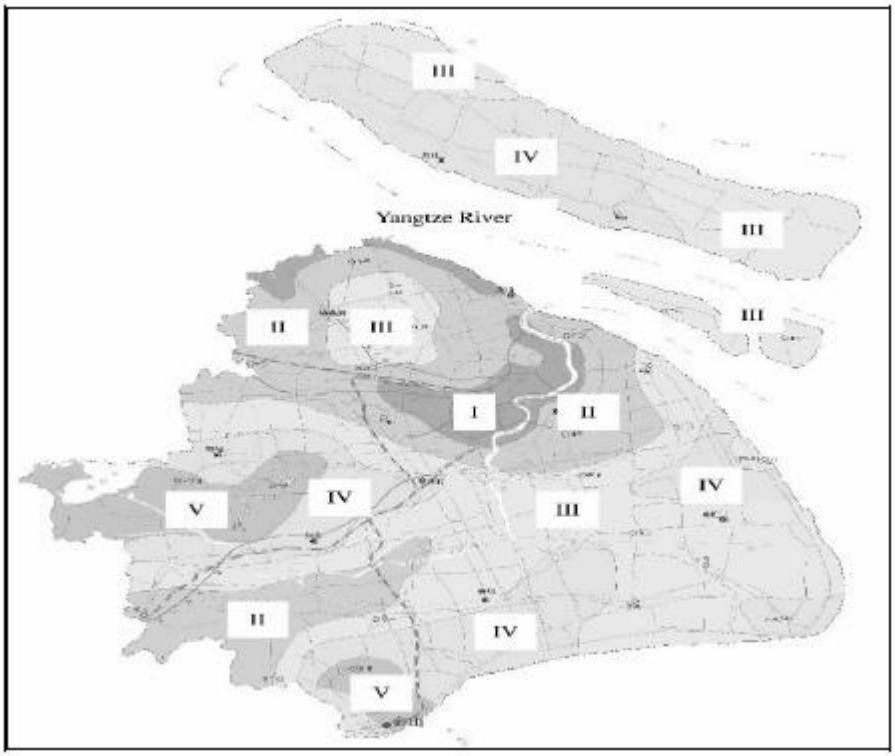

Figure 21: Subsidence rate contours of Shanghai. I. 10-13mm/year II. 5-10mm/year III. 3-5mm/year IV. 1-3mm/year V. <1mm/year (Wei 2006).

Unit	F003		F004		FQL
	1981–1990	1991–2000	1981–1990	1991–2000	1984–2003
Top soil	34.5	2.9	7.5	5.4	–0.3
Unconfined aquifer					
The first aquitard	54.3	11.3	43.4	19.4	Missed
The first confined aquifer	7.9	6.5	25.7	15.6	1.4
The second aquitard					56.3
The second confined aquifer					10.9
The third aquitard	4.4	10.9	4.9	9.2	6.8
The third confined aquifer	18.6	62.1	12.0	64.5	20.0
The fourth aquitard	–19.7	6.3	6.5	–14.3	4.9
The fourth confined aquifer					
The fifth aquitard					

Table 13: Percentage of subsidence contributed by different aquifer layers at different extensometer groups in Shanghai (Zhang et al. 2007).

4.2 Faulting and Groundwater Subsidence

Faults are often present in areas of groundwater subsidence, and even create partial hydrologic barriers, dividing areas into their own subsiding basins (Kreitler, 1977). These structural barriers help to prevent the extension of ground subsidence into other areas. Furthermore, the differing hydrostratigraphic units on each side of the fault, mainly the differing thickness of the units, can influence fault reactivation, leading to differential settlement at the surface. Groundwater from one side of the fault does not directly correspond to depression of groundwater on the other side of the fault, since, as previously mentioned, faults can act as partial hydrologic barriers. Thus, this is a mechanism for differential subsidence at the surface, as only the side of the fault with groundwater drawdown will subside at surface, forcing differential settlement along the fault plane, which may also be seen as fault movement (Kreitler 1977).

Figure 22: Correlation between yearly groundwater drawdown and differential displacement of two faults in western Houston, Texas (Kreitler 1977).

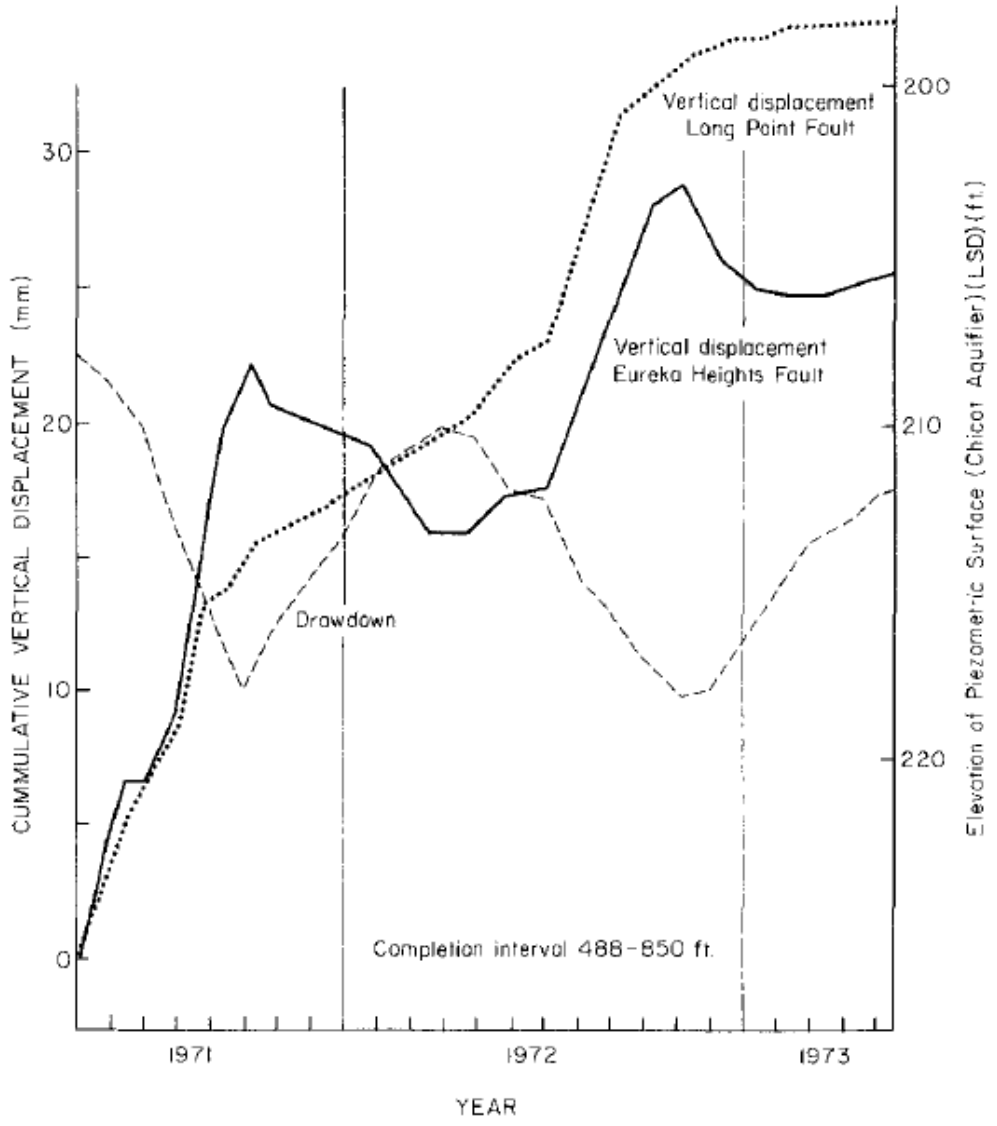

Figure 22 demonstrates cumulative fault displacement with respect to seasonal water drawdown. The Long Point Fault and Eureka Heights fault both increase in cumulative vertical displacement as drawdown from the basin declines, and as drawdown begins to rebound, as occurs with seasonal variations, the fault displacement slows. This confirms a definite correlation, at least in this western Houston aquifer, between fault displacement and groundwater drawdown.

This figure also demonstrates that faults can act as partial hydrologic barriers, since the Eureka Heights fault experiences rebound relative to the other side of the fault, which occurs from a difference in rise of the piezometric surface on each side implying a partial barrier in between (Kreitler 1977).

It may be difficult to deduce whether subsidence along a fault line has been caused by tectonic movement, in which case the fault was active prior to groundwater withdrawal, or if the mechanism is groundwater withdrawal, especially in cases where the downthrow side of the fault is on the same side as the groundwater subsidence. On the other hand, if the fault has reversed from its natural occurrence, as in the current downthrow side was previously the upthrow side, than the mechanism is likely to be due to groundwater withdrawal and the reversal of natural fault slippage is likely due to a difference in compaction on each side of the fault (Kreitler 1977).

Recent research using interferometric synthetic aperture radar (InSAR), which uses satellites to track ground movements, found that faults do act as good subsidence barriers. A study by Amelung et al. (1999), showed that in Las Vegas, which withdraws groundwater from the underlying aquifer at a rate 2 to 3 times greater than it is recharged, subsidence is controlled by quaternary faults to a greater degree than previously thought. The study makes mention of Eglington fault, which not only helps shape the subsidence bowl of Las Vegas, but has been shown, by InSAR, to be a barrier of groundwater and may include less compressible soils on the opposite side of subsidence.

Faults that occur in areas of groundwater withdrawal induced subsidence will influence the shape and magnitude of the subsidence bowl, largely by limiting the area in which groundwater drawdown can occur. As this occurrence may be looked on as beneficial, there can be some drawbacks. Fault planes will be vulnerable to slippage and reactivation by subsidence and may cause damage to buildings and other engineered structures if surface displacement occurs. They also can make prediction of future subsidence rather difficult and unreliable.

4.3 Prediction Methods

Prediction methods that are used to quantify subsidence from groundwater withdrawal differ from those for material extraction, since for groundwater withdrawal there is less stress redistribution occurring. The prediction techniques used for groundwater withdrawal are: statistical methods, 1D numerical calculation method, Quasi-3D methods, 3D seepage model and 3D fully coupled method.

4.3.1 Statistical Methods

There are three statistical methods covered here, the influential function method, Gray theory model and regression analysis method. The influential function method (Holzer and Bluntzer 1984) was the earliest method, and involves finding the deformation time relationship from recorded subsidence data. Regression analysis is also quite simple as it obtains a function of subsidence occurring and groundwater withdrawn to predict yearly subsidence figures, and impose a groundwater withdraw limit. Gray's theory finds a relationship of

factors by comparing them to subsidence; however, it is not very accurate as a prediction technique.

4.3.2 1D Numerical Method

As computer technology took off in the 1970's, it allowed for development of numerical modelling for ground subsidence. However, in the early stages the computing power was not very good, and analysis was limited to only one-dimension. This one-dimensional model was not able to take into account horizontal movements or replenishment of groundwater from inflows. However in a multi-layer system it was able to use consolidation parameters and calculate which aquitard layer was allowing for the most subsidence to occur.

4.3.3 Quasi-3D-Seepage Method

The Quasi-3D-Seepage method consists of two models, the two-step method and the time-step combined model. The two-step method calculates subsidence in two different stages. First, the change in groundwater head is found using a groundwater seepage model, which employs axis-symmetrical assumptions. Second, the consolidation of layers is found using the result of the first step, namely groundwater head, by calculating effective stress and soil deformation with the parameters of coefficient of water storage μ and soil compression coefficient α_v (Chen et al. 2005, in Xu et al. 2007).

In the time-step combined method the two parameters, coefficient of water storage and soil compression coefficient are combined according to the way of coefficient of water storage. This model assumes that water seeps horizontally

and ground consolidates vertically. Li et al. (2000) developed a Quasi-3D model using the governing flow equation:

[8] $$\frac{\partial}{\partial x}\left(T\frac{\partial H_i}{\partial x}\right)+\frac{\partial}{\partial y}\left(T\frac{\partial H_i}{\partial y}\right)=S_s\frac{\partial H_i}{\partial t}+Q_{il}+Q_{is}+Q_{id}-Q_{ir}$$

Where H_i is the water head of each aquifer, Q_{il} is the leaked water from each aquifer, Q_{is} is the released water resulting from soil deformation, Q_{id} is the amount of water withdrawn, Q_{ir} is the amount of water recharged, S_s is the specific storage coefficient and T is the transmissibility coefficient (Xu et al. 2007). There are still flaws with this model, as it does not account for any vertical flow nor anisotropy of the hydrologic parameters of soil.

4.3.4 3D Seepage Model

This model accounts for three-dimensional seepage with only vertical consolidation (Figure 23). Models stemming from this basic concept ultimately use the parameters of hydraulic conductivity, hydraulic head, withdrawal/recharge volume, and the coefficient of specific storage. This method is more advanced mathematically and better suited for prediction of large areas of subsidence than the Quasi-3D model.

Figure 23: Assumed seepage and consolidation for 3D Seepage Model (Xu et al. 2007).

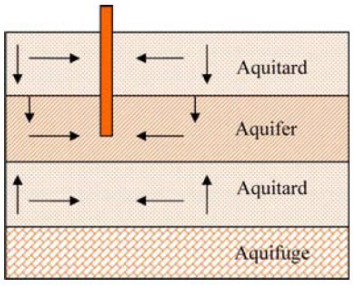

4.3.5 3D Consolidation using Biot's theory model

Prediction of fluid withdrawal subsidence has best been modelled with the use of Biot's theory of consolidation. This theory accounts for the change of effective stress, soil deformation and seepage of excess pore pressure (Xu et al. 2007). One-dimensional modelling using Biot's theory was once the norm for predicting these events, however this method is very limited and has given way to more advanced computer programs that can model in detailed 2-D and even 3-D and can account for more geological variables. The benefits of this theory are that it includes the elasto-plastic relationship while calculating the seepage accurately. However, there are difficulties with this model as it needs accurate geotechnical parameters at many points, which is sometimes unrealistic when trying to use the most economical method (Xu et al. 2007).

4.4 Case study: Venice

Subsidence in Venice, Italy has been caused by excessive groundwater withdrawal resulting in aquitard consolidation. Teatini et al. (1995) reconstructed the underground system of aquifers. There are six aquifers in total that are withdrawn from, which may lead to complex surface subsidence.

A study was conducted by Teatini et al. (1995) to simulate land subsidence in the Venice area as a result of aquitar and aquifer compaction. They used the Quasi 3-D nonlinear flow model for their analysis and also employed a one dimensional vertical consolidation model.

The Quasi 3-D models rely on equation [8] in the form of equation [9] for horizontal flow in the aquifers, together with equation [10] for vertical flow from the aquitards.

[9] $$\frac{\partial}{\partial x}\left[T_{xi}\frac{\partial h_i}{\partial x}\right]+\frac{\partial}{\partial y}\left[T_{yi}\frac{\partial h_i}{\partial y}\right]=S_i\frac{\partial h_i}{\partial t}+q_j-q_{j-1}$$

[10] $$\frac{\partial}{\partial z}\left[K_{zj}(n)\frac{\partial h_j}{\partial z}\right]=S_{sj}(n,\sigma')\frac{\partial h_j}{\partial t}$$

Where qj and qj-1 refer to leakage from the overlying and underlying aquitards, $K_{zj}(n)$ represents vertical permeability and is a function of porosity (n), $S_{sj}(n,\sigma')$ represents the specific elastic storage related to effective stress (σ') and porosity (n). These equations are combined using the aquifer-aquitard boundary as a required continuity of hydraulic head and flux of groundwater, resulting in the following equations to find the porosity (n), the permeability (K) and the specific elastic storage (Ss).

[11] $$n = n_0 - 0.434C_c(1-n)^2\frac{d\sigma'}{\sigma'}$$

[12] $$K_z(n)=K_{z0}\left[\frac{n(1-n_0)}{n_0(1-n)}\right]^m$$

[13] $$S_s(n,\sigma') = \gamma_w\left[0.434C_c\frac{1-n}{\sigma'}+n\beta_w\right]$$

Where m is a material dependant coefficient, γ_w and β_w are the specific weight and compressibility of water respectively.

Teatini et al. (1995) then go on to use the hydraulic head, determined from the above equations, in the one-dimensional consolidation equation:

[14] $$\eta(\Delta t) = \sum_{j=1}^{N}\sum_{k=1}^{M}0.434\gamma_w(1-n)\frac{C_c}{\sigma'}\Delta h_{k,j}\Delta b_{k,j}$$

Where N is the number of aquitards, M is the vertical components of which every aquitard has been discretized, Δb_{kj} is the thickness of *k*th finite element of the *j*th aquitard.

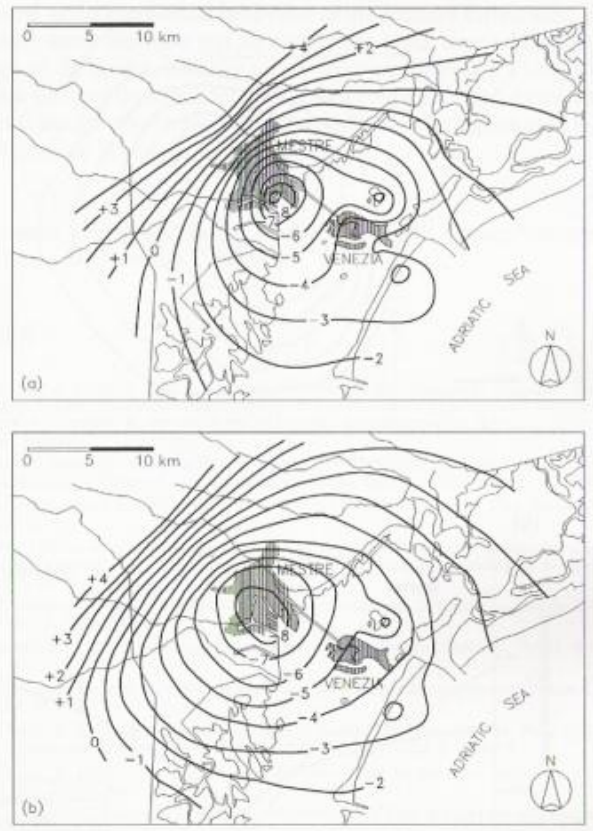

Figure 24: (a) 4th aquifer in 1973 based on piezometer observations. (b) 4th aquifer in 1973 based on flow model (Teatini et al. 1995).

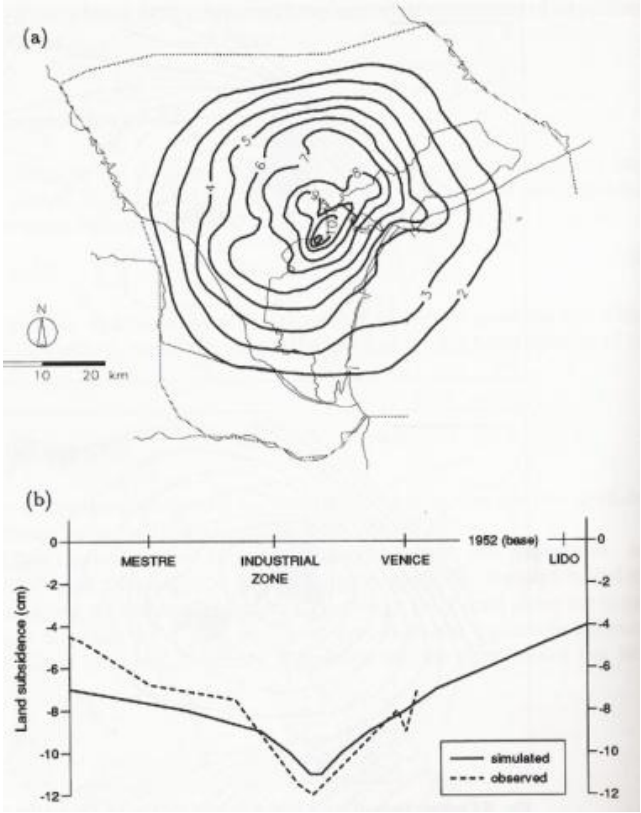

Figure 25: (a) Land Subsidence of Venice from 1952-1973 based on numerical model. (b) Subsidence Profile with simulated and observed results (Teatini at al. 1995).

These parameters and calibration of the model allowed Teatini et al. (1995) to model the drawdown of groundwater in each layer, for example Figure 24 shows minimal differences between observed data and modelled data for the 4th aquifer layer. The results of surface subsidence prediction are shown in Figure 25 and have good correlation with that of the drawdown of groundwater and are also verified by having similar results as the observed data.

5. Subsidence Caused by Hydrocarbon Extraction

Subsidence also occurs from extraction of oil and gas, which is very similar to the type of subsidence that occurs with groundwater extraction. Both extract fluid from the ground which results in a decline in pore fluid pressure, which causes the soil to bear more effective stress, resulting in consolidation of compressible soils and rocks. However, there are some differences between the two, as oil and gas subsidence is usually smaller, but extends over a larger area than the reservoir; this is because oil and gas reservoirs are often located at a greater depth than aquifers. Aquifers on the other hand will generally be close to the surface and the subsidence that occurs will occur right above the depressed water table. Figure 26 shows a typical oil and gas reservoir. Oil and gas reservoirs also are likely to be associated with faults, since deformation needs to occur for the geological trapping mechanism to form, a property that does not often occur with aquifer formation. Thus, faulting is an important mechanism of subsidence, particularly asymmetrical subsidence occurring from oil and gas abstraction.

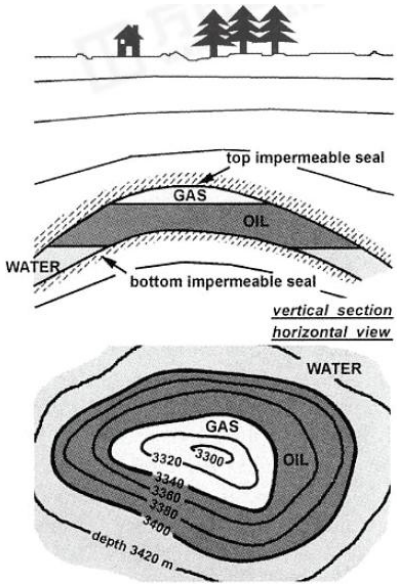

Figure 26: A typical oil/gas reservoir (Gambolati et al. 2006).

5.1 Faulting

Faults originally caused by differential subsidence or pre-existing fault reactivation are an important concern when considering land subsidence, especially in the case of oil and gas extraction. Any slippage of the fault can result in changes of groundwater flow or change the permeability as faults can act as hydrologic barriers, as stated previously with groundwater withdrawal. Displacement of a fault may also result in breakage of the well casing because of displacement or a redistribution of stress. Fault displacement may also propagate to the surface creating undesirable surface displacement which may affect engineered structures.

Pre-existing faults can affect the stress distribution of the reservoir and produce unpredictable surface subsidence results. The extent to which the surface subsidence is altered by an inclined fault depends on a few factors. The depth of the reservoir may prevent the fault from having any significant impact, essentially, the deeper the reservoir the less the importance of the fault. Another influence concerning faults and subsidence due to oil and gas extraction is the orientation of the fault, as it will contribute to the shape of the subsidence bowl (Ferronato et al. 2007).

Ferronato et al. (2007) developed a model which incorporates both faulting and subsidence (see section 5.2). From this model they were able to conduct a sensitivity analysis to show how fault properties affected the subsidence profile at surface by using a two-dimensional model (Figure 27). The fault properties they used were friction angle (φ), fault orientation (β), and reservoir

depth (d). The results of this test are shown in Figures 28-30 and the most unfavourable conditions are shown in Figure 31. As the results show, subsidence at shallow depth causes the highest maximum subsidence as well as differential settlement resulting from the inclined faults. If faulting only occurred on one side of the centre of subsidence, asymmetry would likely result. The fault orientation has only a slight affect on the subsidence profile as Figure 30 demonstrates. However, if the faults were not symmetric on each side, but instead followed a pattern with the same strike and dip, there would be slight asymmetry occurring in the subsidence profile. The friction angle (Figure 31) is limited in its affect on the subsidence profile, especially since the angles (10˚ and 60˚) used are unrealistic as it normally only varies between 25˚ to 35˚. The worst case scenario is shown in Figure 31 with the parameters of d = 500m, $\varphi = 30^{\circ}$, and $\beta = 45^{\circ}$. The following models show symmetrical profiles of subsidence, however if the test model (Figure 27) did not have symmetrical properties (fault orientation, friction angle and an angled reservoir), which is more likely to transpire in real ground conditions, an asymmetrical subsidence profile would occur.

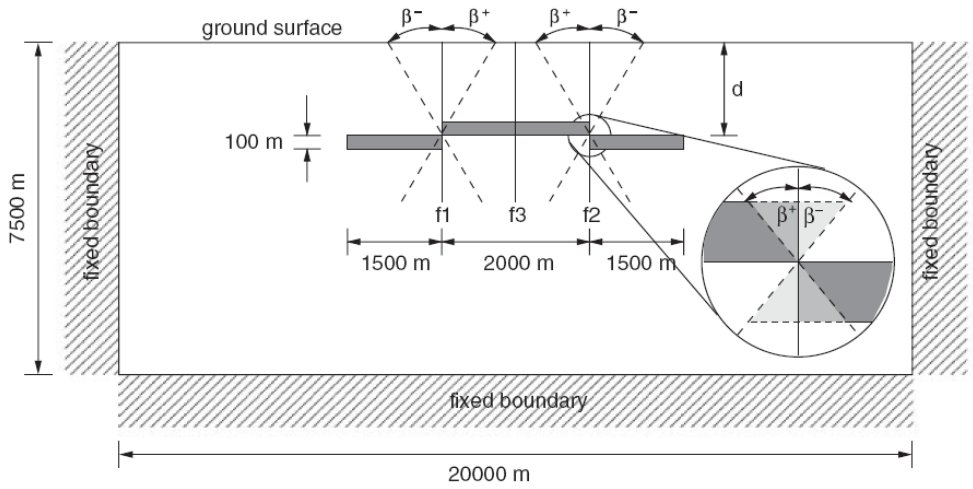

Figure 27: 2-D test diagram for sensitivity analysis with changing (d), (β) and (φ), the grey shaded area are the producing units (Ferronato et al. 2007).

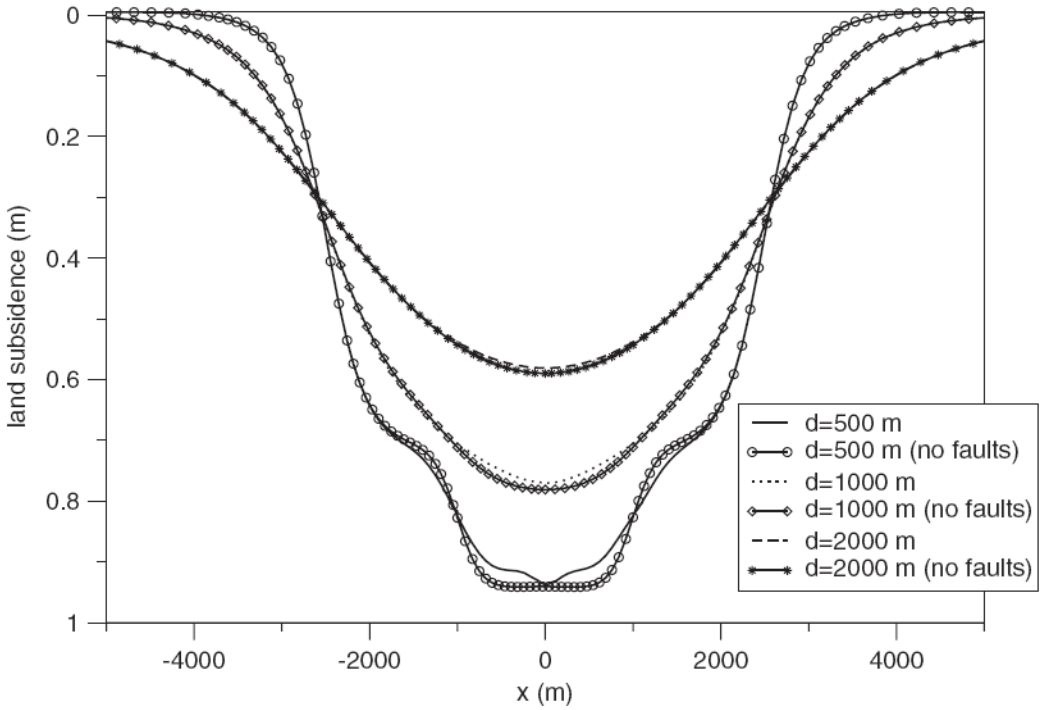

Figure 28: Simulated land subsidence with changing depth (d) = 500m, 1000m, 2000m (Ferronato et al. 2007).

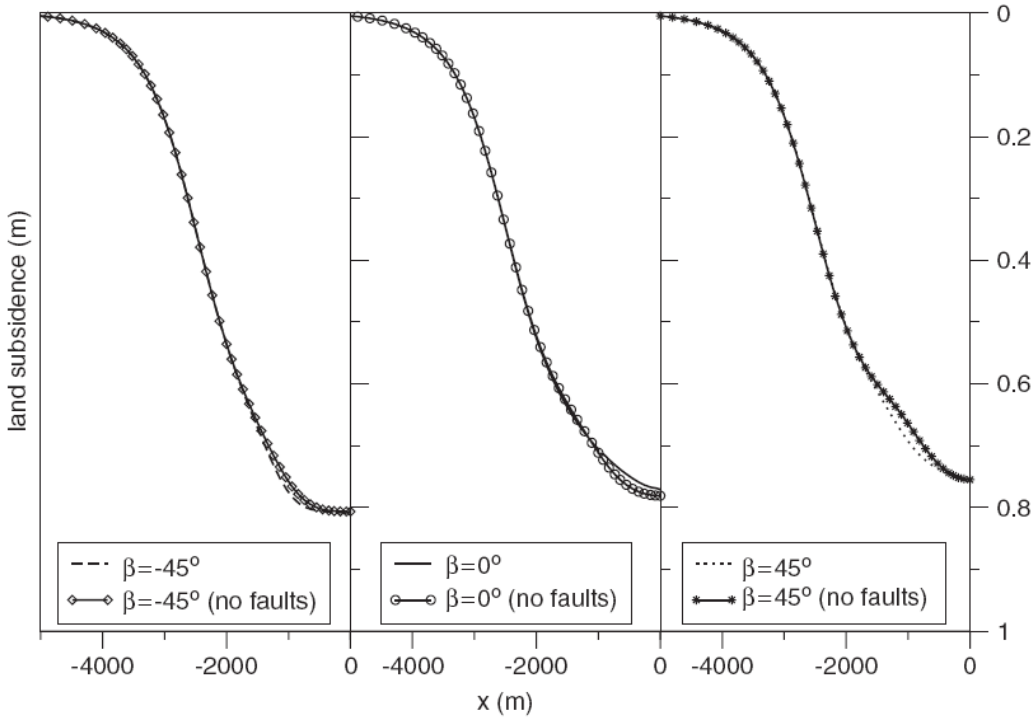

Figure 29: Simulated land subsidence with changing fault orientation (β) = -45˚, 0˚, 45˚ (Ferronato et al. 2007).

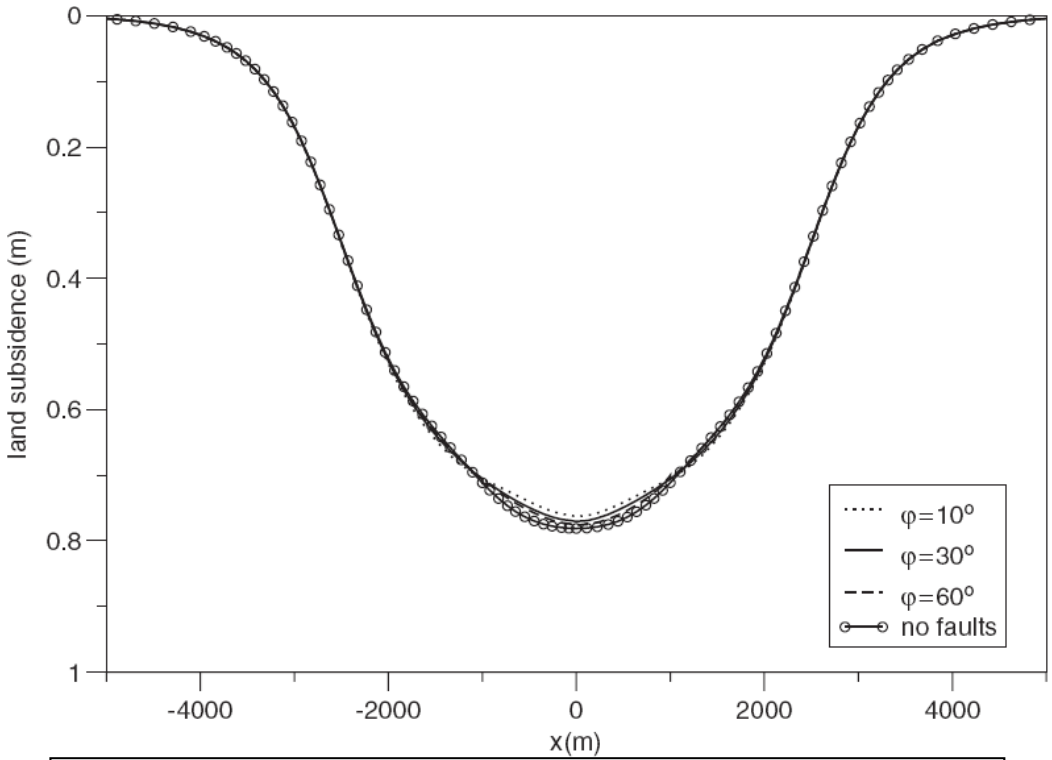

Figure 30: Simulated land subsidence with changing friction angle (φ) = 10˚, 30˚, 60˚ (Ferronato et al. 2007).

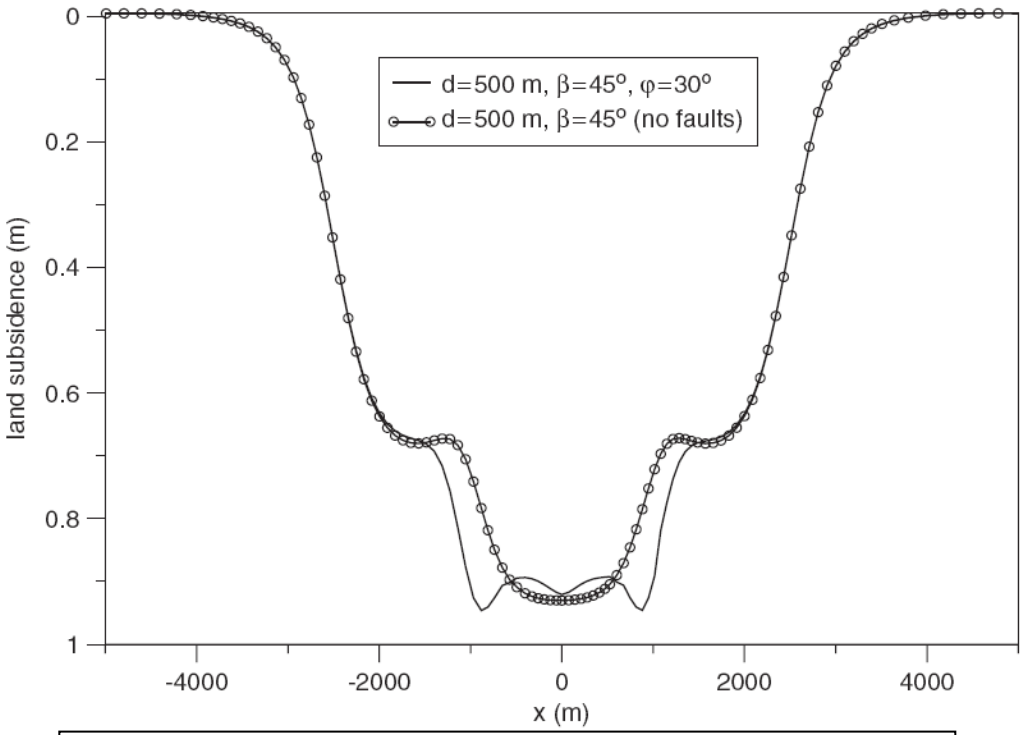

Figure 31: Simulated land subsidence with the worst conditions causing most differential subsidence (Ferronato et al. 2007).

5.2 Prediction Methods

Prediction methods for oil and gas subsidence are very similar to those of groundwater subsidence, which are summarised in section 4.4, since the mechanisms are similar.

There has been some development of new models however that pertain only to oil and gas, as the one used in the sensitivity analysis above. Ferronato et al. (2007) developed a class of linear interface elements and tail interface elements, which have been specifically defined to predict fault movement and opening. These elements are compatible with finite element and have been

incorporated into the prediction of subsidence due to oil and gas withdrawal. The following case study uses this model to replicate a real world example.

5.3 Case Study: Northern Italy Reservoir

Ferronato et al. (2007) applied their subsidence model to a Northern Italy reservoir. The reservoir was 1500 metres in depth, and was intersected by eight faults with an orientation of 0˚. The reservoir thickness runs from 20 metres to 80 metres, in which all faults intersected entirely. The fixed boundaries of the model were assumed to be 20 x 35 kilometres and the depth boundary was 20 kilometres. There is assumed to be no cohesion along the faults and they have a 30˚ friction angle. Pore pressure drawdown over a twenty year span is assumed to be 15 MPa and occurs linearly through time and is fully restored after another twenty years as Figure 32 shows. The area of the reservoir pore pressure drawdown and intersecting faults is shown in Figure 33. The pressure drawdown in the model is applied in 20 two-year time intervals. The constant overburden gradient was 10^{-2} MPa/m and the poisson's ratio was 0.3 over the entire volume. The model computes the slippage and opening of faults as well as the normal and tangential stress at the fault surface, which is shown in Figure 34 for fault 8. The model eventually showed that faulting, at least in the case of this Northern Italian reservoir, does not have a significant impact on land subsidence. The difference between subsidence without faulting and subsidence with faulting is shown in Figure 35 and concludes that of the two faults that were affected by slippage, the maximum subsidence difference is only 0.06 cm. One interesting note here is the

presence of slippage only on the faults at the outer edge of the pore pressure drawdown, as there may be a significant difference in pore pressure across the face of these faults.

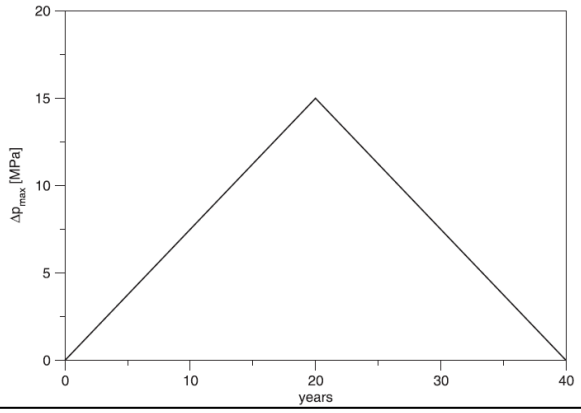

Figure 32: Pore pressure changes during production and after production (Ferronato et al 2007).

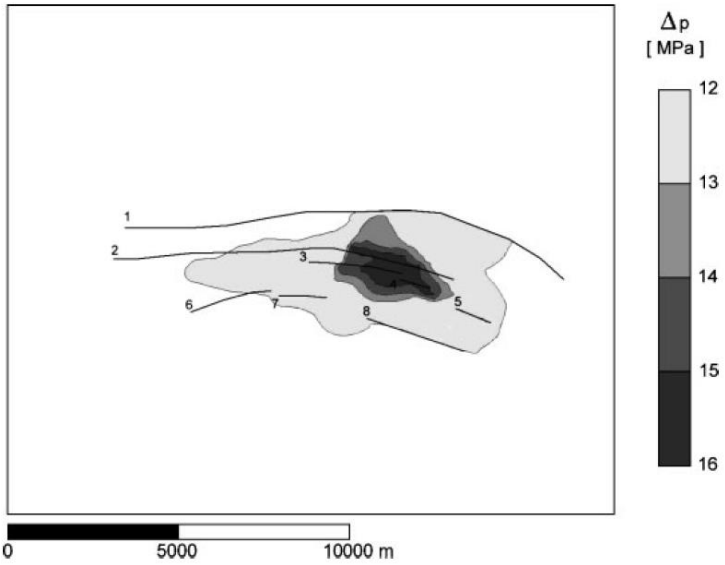

Figure 33: Area of pore pressure drawdown due to reservoir fluid extraction and intersecting faults (Ferronato et al 2007).

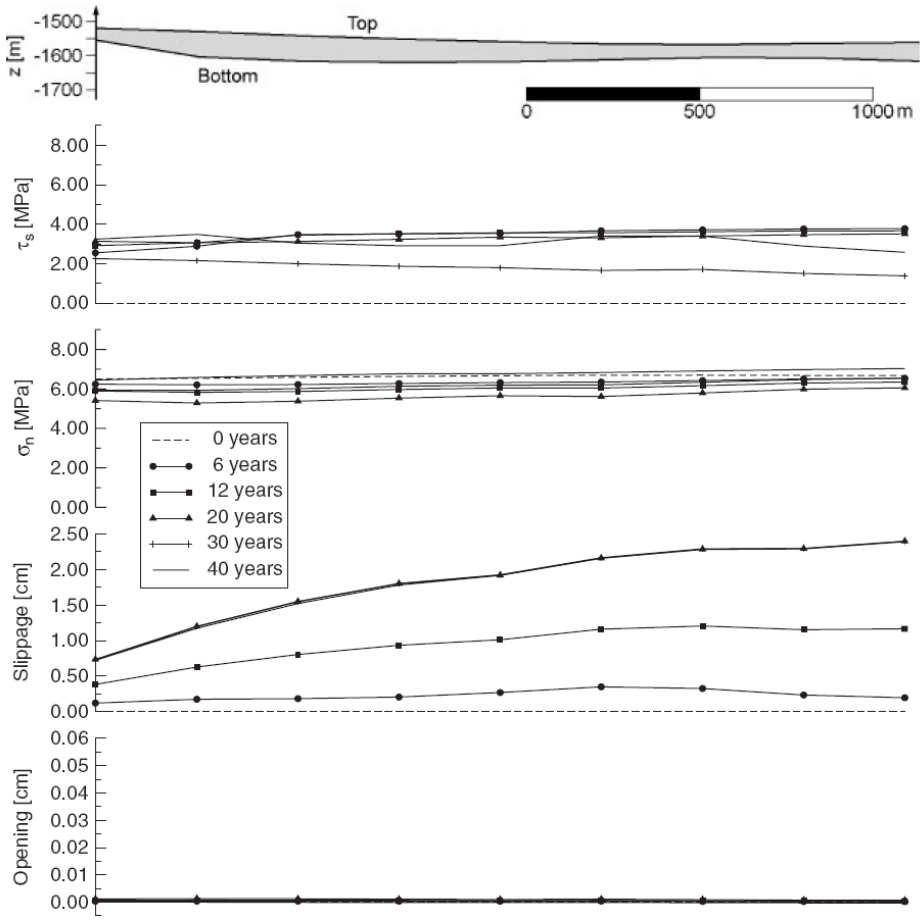

Figure 34: the thickness (z), tangential stress (τ_s), normal stress (σ_n), slippage and opening along fault 8 (Ferronato et al. 2007).

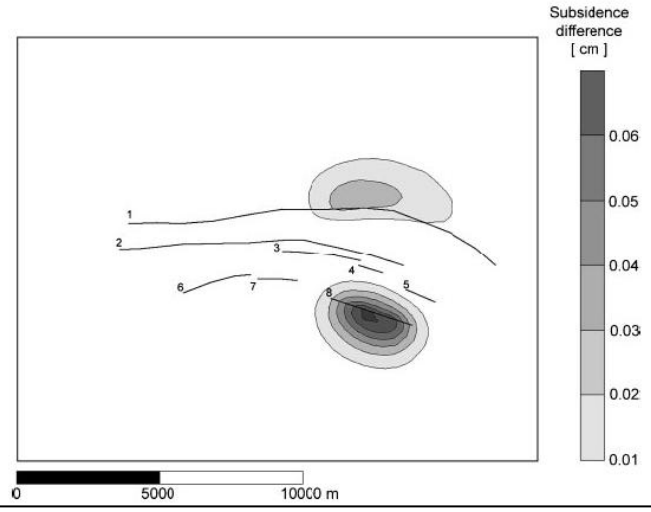

Figure 35: Difference between subsidence with faulting and without faulting (Ferronato et al. 2007).

6. Geothermal Subsidence

Geothermal subsidence is also very similar to subsidence caused by groundwater extraction. The mechanisms of subsidence are essentially the same; there is a decrease in pore pressure due to fluid withdrawal causing soil and rock to consolidate. Prediction and modelling however is very limited in geothermal subsidence because there are not as many cases of subsidence, with most reported cases involving projects in New Zealand. Fortunately, because of the similarities between groundwater and geothermal extraction, researchers that study geothermal subsidence can borrow from examples and studies on groundwater withdrawal and oil and gas induced subsidence.

6.1 Wairakei

One cannot talk about geothermal subsidence without mentioning Wairakei (map shown in Figure 36). Power generation began in 1958 in Wairakei, which is located on New Zealand's north island. The reason that Wairakei is so important to subsidence is because development of its geothermal reservoirs has created more subsidence than any other fluid withdrawal related subsidence, including groundwater and oil and gas (Allis 2000). The reason for this is that little water has been pumped back into the rock until 1990. The maximum subsidence measured in 2001 exceeded 15 metres close to the centre of the subsidence bowl. Horizontal movement rates have also been extensively high reaching 130 mm/year and causing the centre of the subsidence bowl to move south 200 metres over a span of 10 to 20 years (White et al. 2005). Horizontal strain has also led to

fissures at the edge of the subsidence bowl. Another troubling fact is the subsidence occurring in other areas away from the geothermal production area of Wairakei that are hydrogeologically linked. These areas are of concern as they are much closer to urban centres than Wairakei.

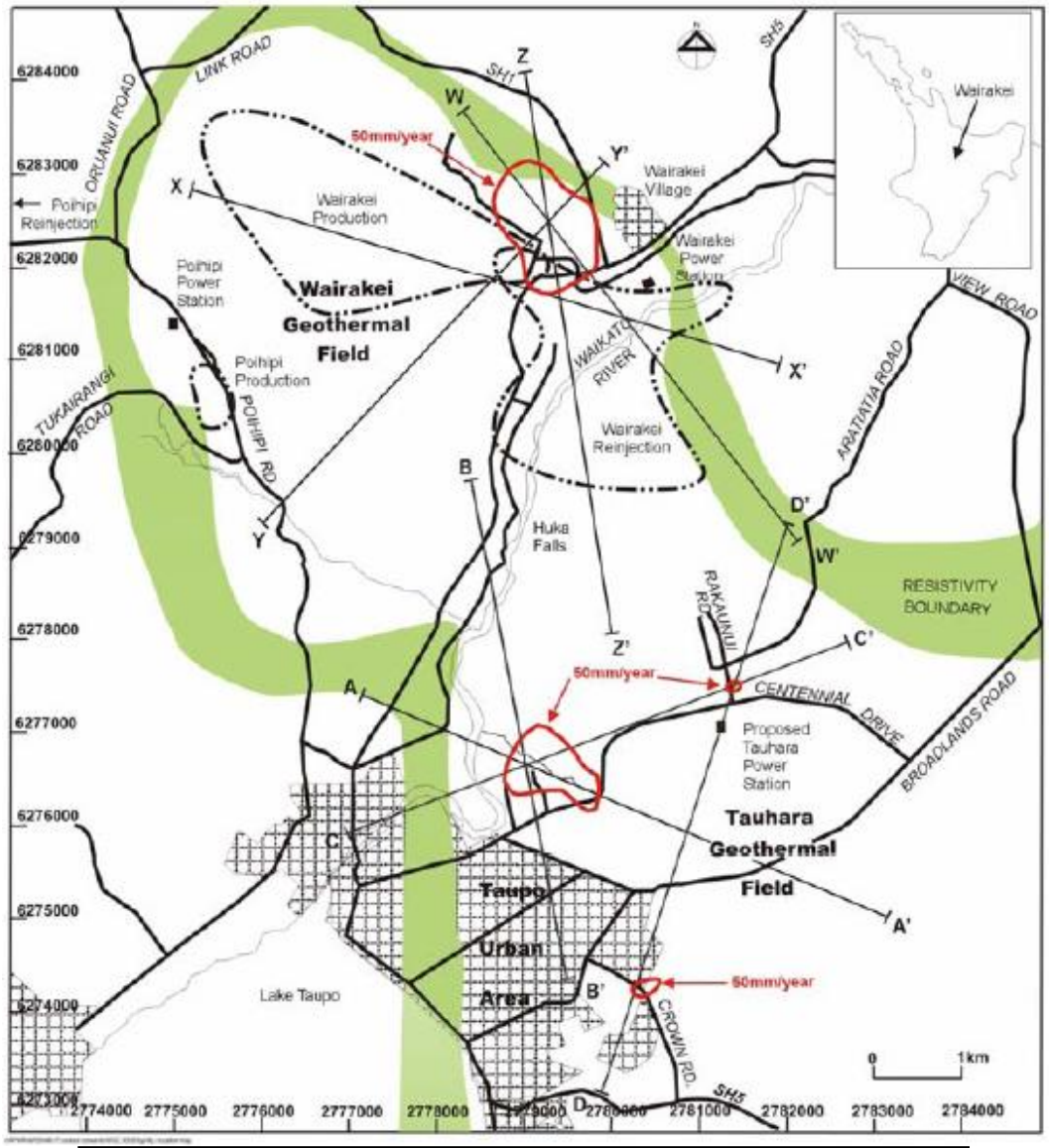

Figure 36: Map of Wairakei and Tauhara Geothermal fields and subsidence bowls outlined in red (White et al. 2005).

The shape of the subsidence bowl at Wairakei (outlined in Figure 36 and Figure 38) is also of great interest because no production wells (located in the

eastern bore field) are located in the bowl. There is also no obvious reason why subsidence would occur in this area (less than 1 km^2) but not extend to other areas closer to where geothermal fluid is being extracted. The compressible layer, which is thought to be a mudstone unit, has no significant change in thickness from the subsidence bowl to the area underneath production wells. Changes in pore pressure also do not significantly change from the eastern bore field to the subsidence bowl. Studies indicate that the most likely source of this displaced subsidence effect is that the compressibility of the mudstone unit responsible for most of the subsidence changes horizontally (Allis 2000). Thus, the compressibility of the layer under the eastern bore field would not be very high compared to this layer underneath the subsidence bowl. Allis (2000) suggests this confined area under the bowl may have been subjected to outflow of boiling water as it was being deposited, creating an area of under-compacted mudstone. However, more recent studies have shown that faults and underlying steep slopes (resulting from old steam vents) of the compacting layer allow water to flow laterally out of the compacting layer into highly permeable interfaces (White et al. 2005). This results in higher subsidence rates as pore pressures drop faster in the compacting layer. The shape of the bowl (Figure 38) and its profile (Figure 37) may then be attributed to the location of these old vents and the compacting layer and any asymmetry might occur because of this.

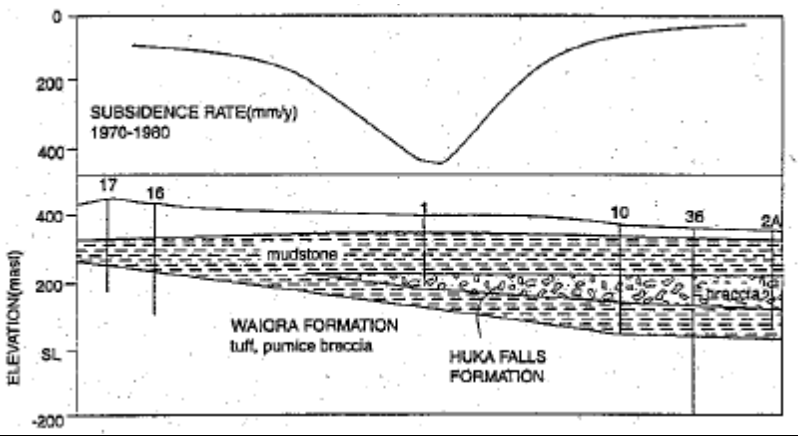

Figure 37: Cross-section of Wairakei subsidence bowl and the subsidence rate along the cross-section (Allis 2000).

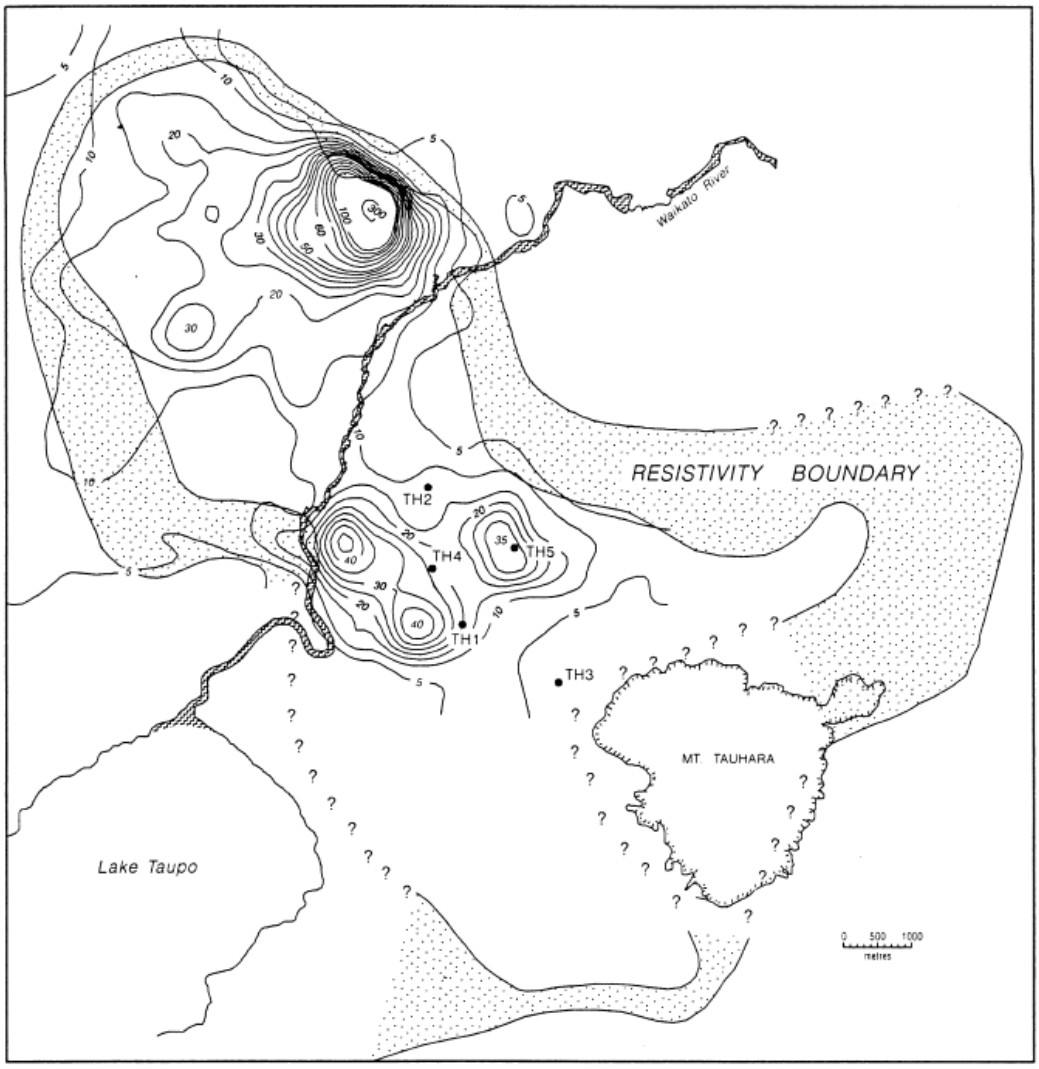

Figure 38: Average subsidence rates through the 1980s and early 1990s at Wairakei and Tauhara geothermal fields (Allis 2000).

6.2 Case Study: Wairakei 2D Model

The 2D model of Wairakei by White et al. (2005) used a single set of geotechnical properties (discounting any anomalies such as pumice breccias and ignimbrite layers) of stress-strain behaviour, permeability, stiffness, void ratio, friction angle and cohesion based on several studies. These parameters were then calibrated using historical subsidence information. Different permeability values were used underneath the subsidence bowl to account for the highly permeable vertical faults and old hydrothermal steam vents (mentioned in 6.1). The 2-D model also allows for the use of Biot theory, thus accounting for non-linearity, plasticity and stress changes. Figure 39 shows the historical data and estimates using the model for future data with some different scenarios of the Wairakei subsidence bowl. Figure 40 show a profile of another emerging subsidence bowl in the Tauhara area (its proximity to Wairakei is shown in Figure 36) due to pressure decline of the same units causing the Wairakei subsidence. The predicted subsidence correlates well with measured data, only it overestimates subsidence slightly. This case study demonstrates that fracture permeability is an important contributing factor for subsidence occurring in geothermal areas because the faults act as conduits for water to flow out of the mudstones since permeability of these units is highly anisotropic.

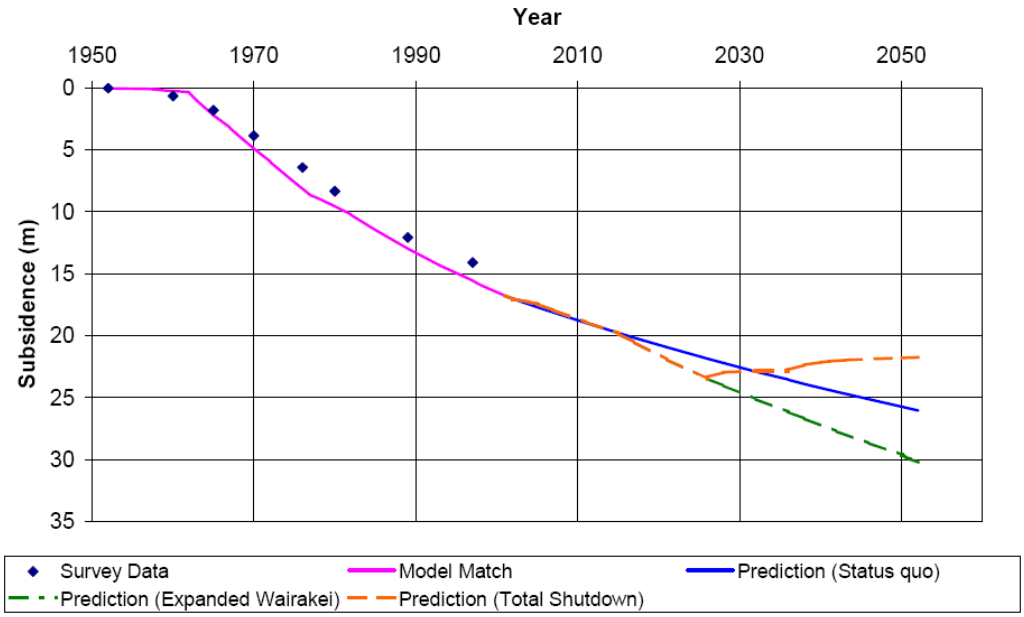

Figure 39: Wairakei subsidence bowl through time (White et al. 2005).

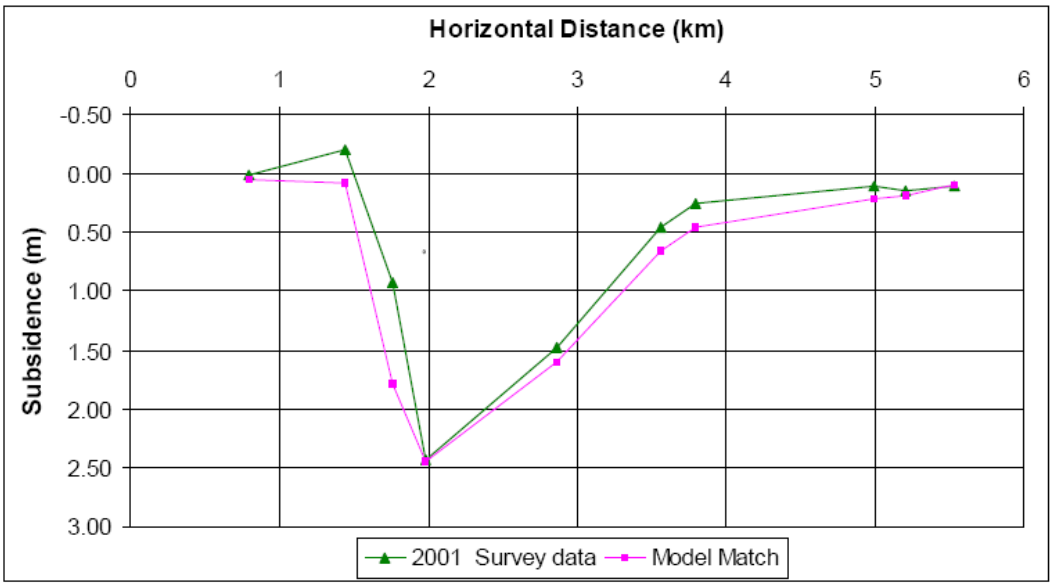

Figure 40: Profile of Tauhara subsidence bowl (White et al. 2005).

7. Conclusion

This overview investigates the causes and contributions to subsidence occurring asymmetrically. Asymmetrical subsidence is concurrent with all five major subsidence causing industries and can be economically devastating to engineered structures at surface. There have been multiple prediction methods aimed to incorporate properties which can lead to asymmetry in the subsidence profile, however it cannot be said with a lot of certainty that any of these models will forward predict very accurately. The following conclusions are made in the five major industries:

Longwall Mining – Asymmetrical subsidence in longwall mining occurs largely due to faulting, but at times also because of surface jointing and the river plain affect. Parameters of faulting such as orientation and distance from the mine opening to the fault will also contribute the shape of the subsidence profile.

Tunnelling – Subsidence can occur in both hard rock and soft rock tunnelling and again disconformities, in particular joint sets, are commonly the cause of abnormalities in the profile. Joint set angles at 0˚ will promote symmetrical subsidence, but as the angle increases the subsidence profile will become increasingly asymmetrical.

Groundwater Withdrawal – Asymmetrical subsidence in groundwater withdrawal is mostly due to soil and rock properties, mainly the thickness and permeability of the compressible layer and the drawdown and flow of pore water pressure. Disconformities may also contribute in this cases, but also act as boundaries to subsidence.

Oil/gas Withdrawal – Subsidence stemming from oil and gas reservoir abstraction may lead to abnormal surface deformation due to faulting, shape of reservoir and rock mass parameters (similar to groundwater withdrawal). However, faulting can be shown to have little to no effect on subsidence, as it largely depends on the fault parameters.

Geothermal – Geothermal subsidence may vary in its control factors of subsidence, as the largest subsidence bowl at Wariakei is largely shaped by fracture porosity, however subsidence may also take place because of leakage from a compressible matrix.

Figure 41 shows typical subsidence troughs from each of the subsidence producing industries presented in this thesis. From this figure it is obvious that subsidence occurs on widely varying scales both in the vertical and horizontal direction. The smallest subsidence trough is produced by tunnelling, as it is barely visible compared to the large subsidence profile created by groundwater extraction. Geothermal production has caused the greatest maximum subsidence of all these industries; however it occurs over a very small area, especially when compared to groundwater and hydrocarbon extraction.

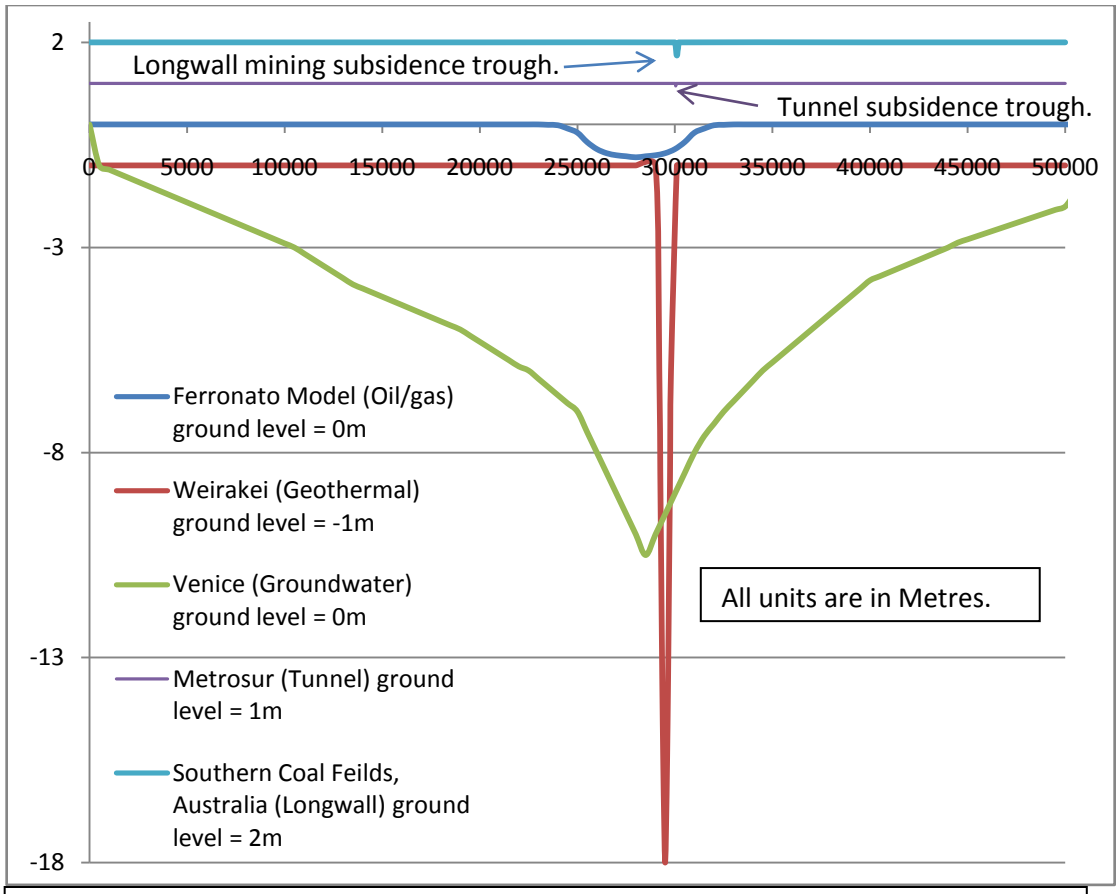

Figure 41: Approximate typical Subsidence troughs of each of the 5 industries presented in this thesis on the same scale (Note: the ground level for each is different).

Although the subsidence caused by these industries does occur at widely varying scales, all of the industries do have some consistencies regarding asymmetrical subsidence, for instance, the effect of discontinuities and variable thickness of compressible units. The determinations of these properties are essential in order to predict asymmetrical subsidence profiles and prevent structural and aesthetic damage to engineered structures.

8. Acknowledgements

The author would like to thank thesis supervisor Erik Eberhardt, together with Kyu Woo, for helping out with this research.

References

Alejano, L.R., Ramirez-Oyanguren, P., Taboada, J., 1999. FDM predictive methodology for subsidence due to float and inclined coal seam mining. International Journal of Rock Mechanics and Mining Sciences, 36:475-491.

Allis, R.G., 2000. Review of subsidence at Wairakei field, New Zealand. Geothermics, 29:455-478.

Amelung, F., Galloway, D.L., Bell, J.W., Zebker, H.A., Laczniak, R.J., 1999. Sensing the ups and downs of Las Vegas: InSAR reveals sctructural control of land subsidence and aquifer-system deformation. Geology, 27.6:483-486.

Atkinson, J.H., and Potts, D.M. 1977. Subsidence above shoallow tunnels in soft ground. Journal of the Geotechnical Engineering Division, ASCE, 103(GT4): 307-325.

Barton, N., Lien, R., Lunde, J. 1974. Engineering classification of rock masses for the design of tunnel support, Rock Mechanics 6, p. 189-236.

Booth, C.J., 2007. Confined-Unconfined Changes above Longwall Coal Mining Due to Increases in Fracture Porosity. Environmental & Engineering Geoscience, Vol. XIII, No. 4:355-367.

Broms, B.B., and Bennermark, H. 1967. Stability of clay at vertical openings. Journal of the Soil Mechanics and Foundations Division, ASCE, 93(SM1): 71-95.

Chen C.X., Cheng J.M., Pei S.P., Liu J. 2005. Numerical model of land subsidence caused by groundwater abstraction and its countermeasure-by example of Suzhou City. Proc 7th Int Symp Land Subsidence (SISLOS 2005) 1:672–679.

Clough, G.W., and Schmidt, B. 1981. Design and performance of excavation and tunnels in soft clay. *In* Soft clay engineering. *Edited by* E.W. Brand and R.P. Bremmer. Elsevier, Amsterdam, The Netherlands. Ch. 8, p. 569–634.

Donnelly, L.J., Culshaw, M.G., Bell, F.G., 2007. Longwall mining-induced fault reactivation and delayed subsidence ground movement in British coalfields. Quarterly Journal of Engineering Geology and Hydrogeology, 41:301-314.

Fang, H.Y., 1997. Introduction to Environmental Geotechnology. CRC Press, 1997, Chapter 15.

Ferronato, M., Gambolati, G., Janna, C., Teatini, P., 2007. Numerical modelling of regional faults in land subsidence prediction above gas/oil reservoirs.

International Journal for Numerical and Analytical Methods in Geomechanics, 2008, 32:633-657.

Galloway, D., Jones, D. and Ingebritsen, S.E. eds, 1999. Land Subsidence in the United States. United States Geological Survey, Circular 1182, p. 177.

Gambolati, G., Teatini, P., Ferronato, M., 2006. Anthropogenic Land Subsidence. Earth Science Frontiers, 13(1):160-178.

Gonzalez, C., and Sagaseta, C. 2001. Patterns of soil deformations around tunnels. Application to the extension of Madrid Metro. Computers and Geotechnics, 28: 445-468.

Harris, D.I., Mair, R.J., Burland, J.B., Standing, J.R., 2000. Compensation grouting to control tilt of Big Ben Clock Tower. *In* Procdedure of the International Symposium on Geotechnical Aspects of Underground Construction in Soft Ground, Kusakabe, Fujita and Miyazaki (eds), Tokyo, Japan.

Holzer T.L., Bluntzer R.L. (1984). Land subsidence near oil and gas fields, Houston, Texas. Ground Water 22(4):450–45.

Institution of Civil Engineers, London, 1977. Ground subsidence. Thomas Telford Limited.1977.

Keilich, W., Seedsman, R., Aziz, N.H., 2006. Numerical Modelling of Mining Induced Subsidence. *In* Coal Operators' Conference:313-326.

Kreitler, C.W., 1977. Fault Control of Subsidence, Houston, Texas. Ground Water, 15.3.

Leca, E., Leblais, Y., Kuhnhenn, K., 2000. Underground Works in Soils and Soft Rock Tunneling. In International Conference on Geotechnical and Geological Engineering. Melbourne, Australia:220-268.

Li Q.F., Fang Z., Wang H.M. (2000). A mathematical model and forecast of groundwater workable reserves for Shanghai. Shanghai Geol 2:36–43 (in Chinese)

Loganathan, N., and Poulos, H.G. 1998. Analytical prediction for tunnelling-induced ground movements in clays. Journal of Geotechnical and Geoenvironmental Engineering, 124(9): 846-856.

Maynar, M.M., Rodriguez, L.M., 2005. Predicted versus measured soil movements induced by shield tunnelling in the Madrid Metro Extension. Canadian Geotechnical Journal, 42:1160-1172.

Melis, M., Medina, Luis., Rodriguez, J.M., 2002. Prediction and analysis of subsidence induced by shield tunnelling in the Madrid Metro Extension. Canadian Geotech. Journal, 39:1273-1287.

Mousavi, S.M., Shamsai, A., El Naggar, M.H., Khamehchian, M., 2001. A GPS-based Monitoring Program of Land Subsidence Due to Groundwater Withdrawal in Iran. Canadian Journal of Civil Engineering,28:452-464

Oteo, C., and Moya, J.F. 1979. Evaluación de parámetros del suelo de Madrid con relación a la construcción de túneles. *In* Proceedings of the 7th European Conference on Soil Mechanics and Foundation Engineering, Brighton, UK. A.A. Balkema, Rotterdam, The Netherlands. Vol. 3, Paper F13, p. 239-247.

Peck, R.B. 1969. Deep excavations and tunnelling in soft ground. *In* Proceedings of the 7th International Conference on Soil Mechanics and Foundation Engineering, Mexico City, 25-29 August 1969. A.A. Balkema, Rotterdam, The Netherlands. Vol. 4, p. 225-290.

Rankin, W.J., 1988. Ground movements resulting from urban tunnelling: predictions and effects. Engineering Geology of Underground Movements, geological Society Engineering geology Special Publication, Bell, F.G., Culshaw, M.G., Cripps, J.C., Lovell, M.A. (eds), No.5:79-92.

Sagaseta, C., Moya, J.F., and Oteo, C. 1980. Estimation of ground subsidence over urban tunnels. *In* Proceedings of the 2nd conference on Ground Movement and Structures, Cardiff, Wales. p. 331-344.

Schmidt, B., 1989. Consolidation settlement due to soft ground tunneling. *In* Proceedings of the twelfth International Conference on Soil Mechanics and Foundation Engineering, Rio de Janiero, Brazil.

Teatini, P., Gambolati, G., Tosi, L., 1995. A new three-dimensional nonlinear model of the subsidence at Venice. *In* Barends, F.B.J., Brouwer, F.J.J., Schroder, F.H., 1995. Land Subsidence. International Association of Hydrological Sciences Publication, 1995, pg. 353-361.

Thompson, T., 2006. Ground Subsidence and Groundwater.

Verruijt, A., and Booker, J.R. 1996. Surface settlements due to deformation of a tunnel in an elastic half plane. Geotechnique, 46(4): 753-757.

Wei, Q. 2006. Land subsidence and water management in Shanghai. Master Thesis, Delft, The Netherlands, 2006.

White, P., Lawless, J., Terzaghi, S., Okada W., 2005. Advances in Subsidence Modelling of Exploited Geothermal Fields. Proceeding World Geothermal Congress 2005.

Whittaker, B.N. and Reddish, D.J., 1989. Subsidence: Occurence, Prediction and Control. Elsevier & Amsterdam, 1989.

Wu, J.H., Ohnishi, Y., Nishiyama, S., 2004. Simulation of the mechanical behaviour of inclined jointed rock masses during tunnel construction using Discontinuous Deformation Analysis (DDA). International Journal of Rock Mechanics and Mining Sciences, 41:731-743.

Xie, H., Yu, G., Yang, L., Zhou, H., 1998. The Influence of Proximate Fault Morphology on Ground Subsidence Due to Extraction. International Journal lf Rock Mechanics and Mining Science, 35(8): 1107-1111.

Xu, Y.S., Shen, S.L., Cai, Z.Y., Zhou, G.Y., 2007. The State of Land Subsidence and Prediction Approaches Due to Groundwater Withdrawal in China. Natural Hazards, 45:123-135.

Yuming, W., 1998. Subsidenc caused by ground-water inflow to the Dayaoshan Railway Tunnel. *In* Land subsidence case studies and current research: Proceedings of the symposium on Land Subsidence. Poland, J.F. (Editor).

Zangerl, C., Evans, K.F., Eberhardt, E., Loew, S., 2008. Consolidation settlements above deep tunnels in fractured crystalline rock: Part 1-Investigations above the Gotthard highway tunnel. International Journal of Rock Mechanics and Mining Sciences, 45:1195-1210.

Zhang, Y., Xue, J.C., Yu, J., Wei, Z.X., Li, Q.F., 2007. Land Subsidence and Earth Fissures due to Groundwater Withdrawal in the Southern Yangtse Delta, China. Environmental Geology, 55:751-762.

Appendix A: Relevant Papers

Aksoy, C.O., Kose, H., Onargan, T., Koca, Y., Heasley, K., 2003. Estimation of limit angle using laminated displacement discontinuity analysis in the Soma coal field, Western Turkey. International Journal of Rock Mechanics and Mining Sciences, 41:547-556.

Anagnostou, G., 2002. Urban tunnelling in water bearing ground – Common problems and soil-mechanical analysis methods. *In* Proc. Of the second international conference on soil structure interaction in urban civil engineering: Planning and Engineering for the cities of tomorrow. Zurich, Switzerland.

Attewell, P.B., 1987. An overview of site investigation and long-term tunnelling-induced settlement in soil. Engineering Geology of Underground Movements, Geological Society Engineering Geology Special Publication, , Bell, F.G., Culshaw, M.G., Cripps, J.C., Lovell, M.A. (eds), No.5:55-61.

Attewell, P.B., Farmer, I.W., Glossop, N.H., 1978. Ground deformation caused by tunnelling in a silty alluvial clay. Ground Engineering, 11.

Avila-Olivera, J.A., and Garduno-Monroy, V.H., 2008. A GPR Study of Subsidence-Creep-Fault Processes in Morelia, Michoacan, Mexico. Engineering Geology, 100:69-81.

Barends, F.B.J., Brouwer, F.J.J., Schroder, F.H., 1995. Land Subsidence. International Association of Hydrological Sciences Publication, 1995.

Barton, N., Harvik, L., Christianson, M., Bandis, S.C., Makurat, A., Chryssanthakis, P., Vik, G., 1986. Subsidence. *In* Proceedings of the 27th Symposium on Rock Mechanics; key to Energy Production. Hartman, H.L. (editor). Society of Mining Engineers: Littleton, Colorado.

Bell, F.G., 1988. Subsidence associated with the abstraction of fluids. Engineering Geology of Underground Movements, Geological Society Engineering Geology Special Publication, No. 5:363-376.

Brighenti, G., 1997. Land subsidence due to groundwater or hydrocarbons withdrawal in environmentally critical areas. *In* Proceedings of the International Symposium on Engineering Geology and the Environment. Marinos, Koukis, Tsiambaos & Stoumaras (editors). Athens, Greece.

Broms, B.B., 1978. Subsidence from Lowering of the Ground Water Level., *In* Evaluation and Prediction of Subsidence,American Society of Civil Engineers, New York, 1979.

Burland, J.B., 1997. Theme Lecture: Subsidence due to Tunnelling and its effects on Buildings. *In* 14th International conference on Soil Mechanics and Foundation Engineering, Taylor & Francis (editors). Hamburg: 2399-2402.

Campbell, J., Kumpel, H.J., Fabian, M., Fischer, D., Gorres, B., Keysers, C.J., Lehmann, K., 2002. Netherlands Journal of Geosciences, 81 (2):223-230.

Corapcioglu, M.Y., 1984. Land Subsidence – A State-of-the-art review. In Fundamentals of Transport Phenomena in Porous Media. Bear, J. And Corapcioglu, M.Y. (editors). Mordinus Nijhoff Publishers.

Cui, X., Miao, X., Wang, J., Yang, S., Liu, H., Song,Y., Liu, H., Hu, X., 1999. Improved prediction of differential subsidence caused by underground mining. International Journal of Rock Mechanics and Mining Sciences, 37:615-627.

Cui, X., Wang, J., Liu, Y., 2001. Prediction of progressive surface subsidence above longwall coal mining using a time function. International Journal of Rock Mechanics and Mining Sciences, 38:1057-1063.

Hejmanowski, R., 1995. Prediction of surface subsidence due to oil or gasfield development. In Proceedings of the fifth international symposium on land subsidence, FISOLS '95:291-300. Netherlands.

Hole, J.K., Bromley, C.J., Stevens, N.F., Wadge, G., 2007. Subsidence in the geothermal fields of the Taupo Volcanic Zone, New Zealand from 1996 to 2005 measured by InSAR. Journal of volcanology and Geothermal Research, 166:125-146.

Holzer, T.L., and Johnson, A.I., 1985. Land Subsidence Caused by Ground Water Withdrawal in Urban Areas. Geojournal, 11.3:245-255.

Howard, H., Steeley, M., 1992. SME Mining Engineering Handbook. Society for Mining, Metallurgy, and Exploration, 1992, p. 955.

Howle, J., Langbein, J., Farrar, C., 2003. Formation near the Casa Diablo geothermal well field and related processes Long valley caldera, Eastern California, 1993-2000. Journal of Volcanology and Geothermal Research, 127:365-390.

Karaman, A., Carpenter, P.J., Booth, C.J., 2001. Type-curve analysis of water-level changes induced by a longwall mine. Environmental Geology, 40:897-901.

Kim, J.M., and Parizek, R.R., 1999. Three-Dimensional Finite Element Modelling for Consolidation Due to Groundwater Withdrawal in a Desaturating Anisotropic Aquifer System. International Journal for Numerical and Analytical Methods in Geomechhanics, 23:549-571.

Lee, K.M., Rowe, R.K., Lo, K.Y., 1992. Subsidence owing to tunnelling. I. Estimating the gap parameter. Canadian Geotech. Journal, 29:929-940.

Mellors, R.J., Boisvert, A., 2003. Deformation near the Doyote Creek Fault, Imperial County, California: Tectonic or Groundwater-related? An Electronic Journal of the Earth Sciences, 4.

Myrianthis, M.L., 1974. Ground Disturbance Associated with Shield Tunneling, in Overconsolidated Stiff Clay. Rock Mechanics, 7.

O'Sullivan, M., Yeh, A., Mannington, W., 2009. History of numerical modelling of the Wairakei geothermal field. Geothermics, 38:155-168.

Poland, J.F., 1979. Subsidence in United States Due to Ground-Water Withdrawal. *In* ASCE Annual Convention and Exposition, Atlanta, Ga.

Rodriguez-Roa, F., 2002. Ground Subsidence due to a Shallow Tunnel in Dense Sandy Gravel. Journal of Geotechnical and Geoenvironmental Engineering, 128,5:428-434.

Rowe, R.K., and Lee, K.M., 1991. Subsidence owing to tunnelling. II. Evaluation of a prediction technique. Canadian Geotech. Journal, 29:945-954.

Sheorey, P.R., Loui, J.P., Singh, K.B., Singh, S.K., 2000. Ground subsidence observations and a modified influence function method for complete subsidence prediction. International Journal of Rock Mechanics and Mining Sciences, 37:801-818.